Table 4 Scores and summary statistics of TWSTRS-severity Scale (patient 2)

	A						B	C	D	E	F	Total
	A1	A2	A3	A4	A5	Total of A 0-12	0-10	0-2	0-3	0-4	0-4	0-35
Numbers of rater	27	27	27	27	27	27	27	27	27	27	27	27
Mean	3.7	1.7	1.0	0.1	0.2	6.6	9.3	1.1	0.9	2.5	3.5	24.0
Standard deviation	0.5	0.7	0.8	0.3	0.4	1.6	1.0	0.4	0.6	0.8	1.3	3.0
Maximum	4	3	2	1	1	9	10	2	2	4	4	30
Minimum	3	0	0	0	0	4	8	0	0	1	0	18
Reference (Mean of 3 raters)	4	2	2	0	0	8	8	1	1	3	4	25

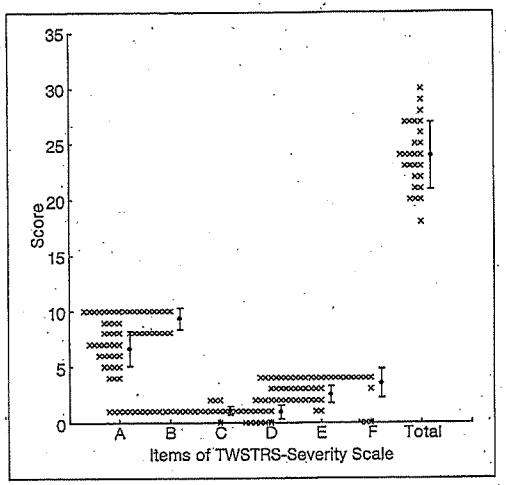

Fig. 2 Score of each rater and summary statistics of the TWSTRS-severity Scale (patient 2)

2．要約統計量の算出

TWSTRS-重症度スケールのスコアを，患者映像別に，Table 3, 4 および Fig. 1, 2 に示した。また，図表には，項目別スコアおよび合計スコアの要約統計量(評価者数，平均値，標準偏差，最大値，最小値）も図示し，さらにエラン社から提供された「正解」も参考として示した。

患者映像 1 の要約統計量を Table 3 および Fig. 1 に示した。その結果，27 人の評価者における TWSTRS-重症度スコアの合計点の平均値は 17.8 点であり，エラン社から提供された「正解」の 18 点とほぼ等しい数値であった。また，A～F の項目ごとの平均値も，エラン社の「正解」とほぼ一致した。

患者映像 2 の要約統計量を Table 4 および Fig. 2 に示した。患者映像 2 における TWSTRS-重症度スコアの合計点の平均値は 24.0 点であり，エラン社から提供された「正解」の 25 点とほぼ等しい数値であった。また，A～F の項目ごとの平均値は，患者映像 1 ほどではないものの，エラン社の「正解」と近い数値であった。

3．評価者間信頼性の検討

TWSTRS-重症度スケールの合計点を用いて，評価者間信頼性の指標として級内相関係数（Intraclass Correlation Coefficient: ICC）とその 95%信頼区間の下限を算出し，Table 5 に示した。なお，エラン社が実施した信頼性試験（評価者数：3 人，患者映像数：10 名）の結果も，参考として示した。その結果，ICC=0.745 (95%信頼区間の下限：0.414) となり，エラン社が外国で実施した信頼性試験の ICC=0.763 とほぼ同様な値であった。

Table 5 Intraclass correlation coefficient of TWSTRS-severity Score

	Intraclass Correlation Coefficient (ICC)	The lower limit of 95% confidence interval
Results of this study	0.745	0.414
Reference	0.763	0.534

Ⅲ. 考　察

巫性斜頸の多様な症候を統一して評価する目的で，いくつかの評価スケールが発表されている。従来多く用いられたのは Tsui 評価スケール[9,10]であり，わが国でも A 型ボツリヌス毒素の治験の際，これを改良した Tsui 変法スケールが用いられた[11,12]。Tsui 変法スケールは，回旋と前後屈を 4 段階から 5 段階とし，体軸の偏倚として側彎も加えられている。しかしながら，これらの評価では痛みなど，しばしば患者の主訴となる症状が評価されないため疾患の重症度を必ずしも反映しているとはいえない。また，患者によっては偏倚として回旋，側屈，前後屈以外に，側方偏倚や前後偏倚といったより複雑な斜頸姿勢を有する場合もある。このような背景のもと，最近の臨床研究ではむしろ，より詳細な評価法である TWSTRS が推奨されている。今回はこの TWSTRS について評価者間信頼性を検討した。

TWSTRS 評価者間信頼性は，27 名の日本人評価者を対象にエラン社が米国で作成した TWSTRS-重症度スケールトレーニングビデオを用いて，本評価のトレーニングおよび評価基準の統一化を行ったうえで実施し，評価者間信頼性の指標としては一般的によく用いられる ICC[8]を用いた。ICC は，評価者間の評価の一致性が高い場合には 1 に近い値をとり，一致性が低くなるにしたがい 0 に近づく係数である。今回の検討結果，ICC=0.745 (95%信頼区間の下限：0.414) となり，エラン社が外国で実施した信頼性試験の ICC=0.763 とほぼ同様な値であった。また，Conski ら[7]が実施した TWSTRS の信頼性試験は，3 名の評価者が 26 名の患者を評価して行われたが，その結果は ICC=0.79 であり，substantial (ICC=0.6-0.8) であるとしている。

以上より，日本においても TWSTRS の十分な評価者間の信頼性が確認できたと考えられた。また，TWSTRS 合計スコアおよび下位項目の平均値がエラン社の基準値と類似していることから，日本と米国の評価の均一性も確認された。

[付記]

TWSTRS 評価者間信頼性検討会参加施設および医師名（順不同，敬称略，所属名は 2002 年 7 月試験実施当時）

北海道大学医学部附属病院リハビリテーション科　中馬孝容，東京大学医学部附属病院神経内科　宇川義一・寺尾安生，東京女子医科大学病院神経内科　大澤美貴雄・村松美由起，東邦大学医学部付属大橋病院臨床検査医学研究室　高宮清之，北里大学東病院神経内科　秋野　裕・梁　正淵，聖マリアンナ医科大学病院神経内科　堀内正浩，信州大学医学部附属病院内科　橋本隆男，寺本神経内科クリニック　寺本　純，武田総合病院神経内科　松本真一・岩崎幸子，奈良県立医科大学附属病院神経内科　田丸　司，近畿大学医学部堺病院神経内科　中村雄作・三浦浩介，関西医科大学附属病院神経内科　伊藤　恒，徳島大学医学部附属病院内科　坂本　崇，産業医科大学病院神経内科　玉川　聡，鹿児島大学医学部附属病院神経内科　宿村公良，弘前大学医学部附属病院神経内科　馬場正之・神成一哉・前田哲也・村上千恵子・大和　博・木村珠容・新井　陽

文　献

1) Nakashima K, Kusumi M, Inoue Y, Takahashi K: Prevalence of focal dystonias in the western area of Tottori Prefecture in Japan. Mov Disord 10: 440-443, 1995
2) Nutt JG, Muenter MD, Aronson A, Kurland LT, Melton LJ: Epidemiology of focal and generalized dystonia in Rochester, Minnesota. Mov Disord 3: 188-194, 1988
3) National Spasmodic Torticollis Association HP: http://www.torticollis.org/
4) Birner P, Schnider P, Wissel J, Muller J, Auff E: Comparison of various treatments for spasmodic torticollis. Subjective rating of effectiveness by patients. Mov Disord 13 Suppl 2: 227, 1998
5) Braun V, Richter HP: Selective peripheral denervation for spasmodic torticollis: 13-year experience with 155 patients. J Neurosurg 97: 207-212, 2002
6) Magar R, Marchetti A, Lau H, Davis T, Brashear A, Watts MW: Treatment of algorithm for cervical dystonia. Mov Disord 15 Suppl 3: 150-151, 2000
7) Conski ES, Lang AE: Clinical assessments of patients with cervical dystonia. In Therapy with Botulinum Toxin. Jankovic J, Hallett M (Eds), Marcel Deckker, New York, 1994, pp211-237
8) Fleiss JL: The Design and Analysis of Clinical Experiments. John Wiley & Sons, New York, 1986, pp26-28
9) Tsui JKC, Eisen A, Mak E, Carruthers J, Scott A, Caine DB: A pilot study on the use of botulinum toxin

in spasmodic torticollis. Can J Neurol Sci 12: 314-316, 1985
10) Tsui JKC, Eisen A, Stoessi AJ, Caine S, Caine DB: Double-blind study of botulinum toxin in spasmodic torticollis. Lancet ii: 245-247, 1986
11) 目崎高広, 梶　龍兒, 木村　淳, 納　光弘, 水野美邦, 他: A型ボツリヌス毒素製剤 AGN191622 の痙性斜頸および顔面痙攣に対する有効性の検討（第II相多施設共同試験）. 脳神経 47: 749-754, 1995
12) 目崎高広, 梶　龍兒, 木村　淳, 萬年　徹: A型ボツリヌス毒素製剤 AGN191622 の痙性斜頸に対する用量反応関係の検討（第II相試験）. 脳神経 47: 857-862, 1995

Toxicon 55 (2010) 407–414

Contents lists available at ScienceDirect

Toxicon

journal homepage: www.elsevier.com/locate/toxicon

Quantitative determination of biological activity of botulinum toxins utilizing compound muscle action potentials (CMAP), and comparison of neuromuscular transmission blockage and muscle flaccidity among toxins

Yasushi Torii [a,b,*], Yoshitaka Goto [a], Motohide Takahashi [c], Setsuji Ishida [c], Tetsuhiro Harakawa [a], Takashi Sakamoto [d], Ryuji Kaji [e], Shunji Kozaki [b], Akihiro Ginnaga [a]

[a] The Chemo-Sero-Therapeutic Research Institute (KAKETSUKEN), 1-6-1 Okubo, Kumamoto-shi, Kumamoto 860-8568, Japan
[b] Department of Veterinary Sciences, School of Life and Environmental Sciences, Osaka Prefecture University, 1-18 Rinku-oraikita, Izumisano, Osaka 598-8531, Japan
[c] Department of Bacterial Pathogenesis and Infection Control, National Institute of Infectious Diseases, 4-7-1 Gakuen, Musashimurayama-shi, Tokyo 208-0011, Japan
[d] Department of Neurology, National Center Hospital of Neurology and Psychiatry, 4-1-1 Ogawa-Higashi, Kodaira-shi, Tokyo 187-8551, Japan
[e] School of Medicine, The University of Tokushima Faculty of Medicine, 18-15 Kuramoto-cho, Tokushima-shi, Tokushima 770-8503, Japan

ARTICLE INFO

Article history:
Received 15 June 2009
Received in revised form 18 August 2009
Accepted 15 September 2009
Available online 22 September 2009

Keywords:
Botulinum toxin
CMAP
Mouse ip LD_{50}
Neuromuscular transmission

ABSTRACT

The biological activity of various types of botulinum toxin has been evaluated using the mouse intraperitoneal LD_{50} test (ip LD_{50}). This method requires a large number of mice to precisely determine toxin activity, and so has posed a problem with regard to animal welfare. We have used a direct measure of neuromuscular transmission, the compound muscle action potential (CMAP), to evaluate the effect of different types of botulinum neurotoxin (NTX), and we compared the effects of these toxins to evaluate muscle relaxation by employing the digit abduction scoring (DAS) assay.
This method can be used to measure a broad range of toxin activities the day after administration. Types A, C, C/D, and E NTX reduced the CMAP amplitude one day after administration at below 1 ip LD_{50}, an effect that cannot be detected using the mouse ip LD_{50} assay. The method is useful not only for measuring toxin activity, but also for evaluating the characteristics of different types of NTX. The rat CMAP test is straightforward, highly reproducible, and can directly determine the efficacy of toxin preparations through their inhibition of neuromuscular transmission. Thus, this method may be suitable for pharmacology studies and the quality control of toxin preparations.

1. Introduction

Clostridium botulinum produces toxins that have been classified into 7 serotypes, A–G, based on their immunological characteristics (Sakaguchi, 1983). The toxins act on neuromuscular junctions and induce muscle relaxation by inhibiting acetylcholine release (Sakaguchi, 1983; Jahn and Niemann, 1994). The toxins cause muscle flaccidity, and have recently been utilized to treat spasm in myotonus and dystonia (Jankovic, 2004). Type A and B toxins were approved as drugs for treatment, and are clinically applied. Type C, E, and F toxins have been used in clinical studies (Mezaki et al., 1995; Eleopra et al., 1997, 1998, 2004). The toxins cleave SNARE proteins (i.e., SNAP-25, synaptobrevin, and syntaxin), which fuse to the synaptic vesicle and nerve cell membrane, blocking neuromuscular transmission by inhibiting the release of acetylcholine from synaptic vesicles. The different types of toxin are selective for specific SNARE proteins. Type A and E toxins cleave SNAP-25, type B toxin cleaves synaptobrevin II, type C toxin cleaves syntaxin and SNAP-25, and type D, F, and G toxins cleave synaptobrevin I and II. The cleavage sites for each toxin differ, even when toxins cleave the same protein (Montecucco and Schiavo, 1994; Schiavo et al., 2000).

The biological activity of botulinum toxins has been evaluated using the mouse intraperitoneal (ip) LD_{50} test (Pearce et al., 1994). This method is not an assessment of toxin efficacy, which is the inhibition of neuromuscular transmission, but of lethality due to respiratory muscle paralysis caused by the toxin. In this method, the results vary due to the individual sensitivity of mice against toxins, and many mice are required to ensure sufficient accuracy levels for the quality control of preparations. Therefore, the method has posed a problem with regard to animal welfare. International meetings on alternative methods for animal testing have been held, and replacements for the mouse ip LD_{50} test have been discussed (Straughan, 2006). The 3 Rs (refinement, reduction, and replacement) have been proposed for alternative methods, and alternative *in-vitro*, *ex-vivo*, and *in-vivo* test systems have been investigated. The *in-vitro* test system, ELISA, determining the endopeptidase activity, does not use animals, but the sensitivity is lower than the mouse bioassay (Hallis et al., 1996; Wictome et al., 1999). This method could determine only light-chain activity in many cases, and the inaccurate determination of toxin function has been reported. The *ex-vivo* test system using the mouse phrenic nerve-hemidiaphragm is sensitive, but it requires a skilled technique, and has a low reproducibility (Bigalke et al., 2001; Yoneda et al., 2005). The *in-vivo* test systems, such as the digit abduction scoring (DAS) and local flaccid paralysis assays, use scores for evaluation (Aoki, 2001; Takahashi et al., 1990; Sesardic et al., 1996). The methods of evaluation involved scoring, and so they have a disadvantage in that the obtained data are discrete quantities. As each test systems has disadvantages; no alternative method has been established.

We attached a greater importance to the following point in devising an alternative method to determine the activity of botulinum toxin: The potency of botulinum toxin should be evaluated based on their pharmacological effect of inhibiting neuromuscular transmission, and not based on their lethal activity, as in the mouse ip LD_{50} assay. There are several test systems to evaluate the inhibition of neuromuscular transmission, and we focused on the measurement of the compound muscle action potential (CMAP) used for the diagnosis of various nervous disorders. The CMAP is generated by the contraction of muscle fibers; the microcurrent generated by muscle contraction is amplified and recorded. Botulinum toxin affects nerve endings to suppress neurotransmission. Therefore, by determining the CMAP amplitude, the action of the toxin suppressing the transmission of electric stimulation to the muscle can be shown numerically. CMAP measurement is utilized by the extensor digitorum brevis (EDB) test, which checks the response to the toxin before treatment in patients who might have antibodies to the botulinum toxin (Kessler and Benecke, 1997). It was reported that the CMAP amplitude was measured in the rat gastrocnemius muscle which was injected several times with botulinum toxin (Cichon et al., 1995). The CMAP amplitude decreased as the toxin activity increased, but quantitative determination of the toxin was not carried out.

In this study, based on this previous CMAP study, we investigated the quantification of biological activity (effect of neuromuscular transmission blockage) by different types of botulinum toxin. We also compared toxins with an inhibitory effect on neuromuscular transmission. In addition, we investigated the muscle flaccidity-inducing effect of the toxins, compared CMAP data, and the overall effect of the toxins.

2. Materials and methods

2.1. Preparation of toxin

Botulinum neurotoxin type A, B, C, C/D, D, E, and F (150 kDa, NTX) were prepared using modified culture and purification methods, as previously reported (Sakaguchi et al., 1981). *C. botulinum* type A A2, type B Okra, type C CB-19, type C/D 003-9, type D 1873, type E 35396, and type F Langeland were used. For type A, B, E, and F organisms, PYG medium containing 2% peptone, 0.05% yeast extract, 0.5% glucose, and 0.025% sodium thioglycolate was used. For type C, C/D, and D organisms, a basic medium containing 0.8% glucose, 0.5% starch, 1.0% yeast extract, 1.0% ammonium sulfate, and 0.1% cysteine hydrochloride salt was used, and cooked meat (6 g) and 0.5% calcium carbonate were added to 100 mL of the basic medium. The organisms were cultured by allowing them to stand at 30 or 37 °C for 2–3 days. Culture fluid was purified by acid precipitation, protamine treatment, ion-exchange chromatography, and gel filtration of M toxin. M toxin was adsorbed to a DEAE Sepharose column equilibrated with 10 mM phosphate buffer, and eluted with a 0–0.3 M NaCl gradient buffer for NTX and non-toxic protein separation. Each NTX was stored at −70 °C until use.

2.2. Experimental animals

Female ICR/CD-1 mice (4 weeks of age, about 20 g, Charles River Laboratories Japan, Yokohama, Japan) and female S/D rats (8 weeks of age, about 200 g, Charles River Laboratories Japan, Yokohama, Japan) were used for the LD_{50} and CMAP tests, respectively. Animals were maintained under controlled light/dark conditions and had free access to food and water. This study was performed in accordance with the guidelines concerning experimental animals established by the Japanese Pharmacological Society, and was approved by the Animal Ethics Committee of our institute.

2.3. Toxin activity (mouse ip LD_{50}) measurements

The LD_{50} of each NTX was determined following ip injection into mice (Pearce et al., 1994). Seven doses with a dilution factor of 1.25 were used to determine the LD_{50}, and 20 animals were used per dose. Mice were evaluated for the first 96 h after administration, and the LD_{50} was calculated by the probit method.

* Corresponding author at: Human Vaccine Production Department, The Chemo-Sero-Therapeutic Research Institute (KAKETSUKEN), 1-6-1 Okubo, Kumamoto-shi, Kumamoto 860-8568, Japan. Tel.: +81 96 344 1211; fax: +81 96 345 1345.
E-mail address: torii-ya@kaketsuken.or.jp (Y. Torii).

0041-0101/$ – see front matter © 2009 Elsevier Ltd. All rights reserved.
doi:10.1016/j.toxicon.2009.09.005

2.4. CMAP measurements

The different types of NTX were serially diluted with physiological saline containing 0.5% human serum albumin. The following dilutions were prepared: 0.1–300 ip LD_{50}/mL type A; 100–1 × 10^5 ip LD_{50}/mL type B, 1–10,000 ip LD_{50}/mL type C, 0.3–100 ip LD_{50}/mL type C/D; 300–1 × 10^5 ip LD_{50}/mL type D, 1–3000 ip LD_{50}/mL type E, and 10–10,000 ip LD_{50}/mL type F. Rats were anesthetized with an ip injection of pentobarbital sodium (Kyoritsu Seiyaku, Tokyo, Japan). After the eyelid reflex disappeared, the left hind leg was shaved, and 0.1 mL of an NTX dilution was injected into the gastrocnemius muscle of five animals.

The CMAP was measured using a Nicolet Viking Quest (Viasys Healthcare, Tokyo, Japan). Rats were anesthetized and fixed in the prone position. The electrode employed was an alligator clip lead wire (Viasys Healthcare, Tokyo, Japan). The stimulating electrode was placed on the root of the spinal cord, the recording electrode was positioned on the belly muscle of the left hind gastrocnemius muscle, the reference recording electrode was placed on the left hind gastrocnemius tendon, and the earth electrode was positioned on the tail root. Electric stimulation was given at 25 mA for 0.2 ms. The CMAP of anesthetized rats was measured before (0) and 1, 2, 4, 7, and 14 days after administration.

To investigate whether the CMAP amplitude can accurately reflect the inhibition of neuromuscular transmission by botulinum toxin, we evaluated muscle relaxants with different mechanisms of action, nondepolarizing neuromuscular blocking drug, d-tubocurarine (d-Tc, Wako, Osaka, Japan), and a depolarizing neuromuscular blocking drug, succinylcholine (SCC, Wako, Osaka, Japan). d-Tc is an antagonist of nicotinic neuromuscular acetylcholine receptors, and provides muscle relaxation by competitive inhibition of acetylcholine. SCC is binding to the nicotinic acetylcholine receptor, and is opening of the receptor's nicotinic sodium channel; a disorganized depolarization of the motor end plate occurs. SCC is not hydrolyzed by acetylcholinesterase, and occurs to persistent depolarization. The receptor's nicotinic sodium channel is inactivated. When acetylcholine binds to an already depolarized receptor it cannot cause further depolarization. As a result, SCC provides muscle relaxation. So, d-Tc and SCC are relaxed muscle by neuromuscular transmission inhibitory as botulinum toxin. d-Tc and SCC were serially diluted 3-fold to yield 0.1–0.9 and 1–9 mg/mL, respectively. Each drug dilution (0.1 mL) was injected into caudal vein of five animals. Electrodes were attached as described above, and the CMAP amplitude was measured for the left hind leg of each rat at 3 and 2 min after d-Tc and SCC administration, respectively. The rats underwent the insertion of a tracheal tube to maintain respiration after drug administration. The respirator was delivered by SN-480-7 (Shinano manufacturing Co., Tokyo, Japan). Tidal volume was set on the respirator at 2 mL and respiratory frequency at 70 breaths/min.

2.5. Digit abduction scoring assay (DAS assay)

The different types of NTX were compared using the DAS assay (Aoki, 2001), which has been reported to assess the muscle flaccidity-inducing effect of botulinum toxin preparations. In the assay, mice received toxin injection into the gastrocnemius muscle, and the muscle flaccidity-inducing effect of the toxin was determined by the degree of digit abduction. The peak DAS responses were observed on Day 2 or 3 post-injection. The DAS assay was modified for rats, and carried out two days after NTX administration. For negative control, rats were injected with dilution solution (physiological saline containing 0.5% human serum albumin). Rats were suspended by the tail, and the degree of digit abduction in the toxin-treated leg was scored on a 5-point scale by an observer who was masked as to the treatment: score 0 = normal leg extension, and digit abduction equivalent to the contralateral side; score 1 = normal leg extension, but digit abduction differed from the contralateral side or two digits in contact while the other digits completely abducted; score 2 = leg extended, but weak abduction of all digits or three digits in contact; score 3 = leg extended without digit abduction, or leg bent with four digits in contact; score 4 = leg bent with no digit abduction.

2.6. Statistical analysis

The waveforms of a single CMAP were converted to 2000 dots using electromyograph software, and the coordinates of the dots were converted to numbers. The distance between the top and bottom of the waveform was measured as the CMAP amplitude. Statistical analysis for neurotoxin (SAN, ver. 1.07, self made soft) was used to analyze the CMAP amplitude. SAN was created to store raw data of the CMAP amplitude and perform various statistical analyses (i.e., *t*-test, regression analysis, parallel line analysis, and correlation coefficient).

For time course of CMAP amplitude, the MULTTEST procedure of contrast statement was performed using SAS (ver. 9.1).

To determine whether the inhibitory effect on the neuromuscular transmission of each NTX was quantifiable, ip LD_{50} data were plotted versus CMAP amplitudes, and the linearity of the regression line was confirmed by regression analysis.

To evaluate the efficacy of each NTX, the regression line of each NTX was calculated for the peak of the effect, as identified above. Regression lines were used to calculate the doses causing 50% (injection site) and 20% (contralateral site) reductions in the CMAP amplitude, and these values were termed the Effective Dose 50 (ED_{50}) and Toxic Dose 20 (TD_{20}), respectively.

For d-Tc and SCh of the data, the Jonckheere–Terpstra trend test was performed using SAS (ver. 9.1).

3. Results

3.1. Dose-dependent effects of the different NTX types on the CMAP amplitude

The CMAP amplitude was measured to compare the inhibition of neuromuscular transmission at the site of toxin administration. In all types of NTX, the CMAP amplitude decreased depending on the concentration of the ip LD_{50}. Following the administration of type B, C, C/D, and D NTX, the CMAP amplitude in the left hind leg was reduced for four days at all dose, and was recovered thereafter at type B of or more 30 ip LD_{50}, type C and type C/D of all dose and type D of 100–10,000 ip LD_{50}. Following type A, E, and F NTX administration, the CMAP amplitude was reduced for two days and recovered thereafter at type A of 0.03–3 ip LD_{50}, type E of or more 1 ip LD_{50}, and type F of or more 10 ip LD_{50} (Fig. 1). After the administration of type A, B, C, C/D, D, and F NTX, the CMAP amplitude in the contralateral leg was reduced for four days at type A of more 3 ip LD_{50}, type B of 10,000 ip LD_{50}, type C of or more 30 ip LD_{50}, type C/D of or more 3 ip LD_{50}, type D of 100,000 ip LD_{50}, and type F of or more 3000 ip LD_{50}, and subsequently recovered at type A of 10 ip LD_{50}, type B of or more 3000 ip LD_{50}, type C of 300 ip LD_{50}, type C/D of or more 3 ip LD_{50}, type D of 100,000 ip LD_{50}, and type F of 10,000 ip LD_{50}, respectively. Following type E NTX administration, the CMAP amplitude was reduced for two days at or more 100 ip LD_{50} and recovered thereafter at 300 ip LD_{50} (Fig. 2).

3.2. Analysis of the CMAP amplitude after the different NTX types were administered

Type A, C, C/D, and E NTX reduced the CMAP amplitude in the toxin-injected limb below 1 ip LD_{50} one day after administration. Regression analysis revealed that the CMAP amplitude for type A, B, C, C/D, and D of NTX on days 1, 2, 4, 7, and 14 and type E and F of NTX on days 1, 2, and 4 following administration was related to the LD_{50} concentrations dose-dependently, and linearity was noted when the logit-transformed CMAP amplitude was plotted against the log ip LD_{50}. Although each NTX varied regarding its LD_{50} value for the reduction of the CMAP amplitude, the linearity range of all types of NTX was from the minimum ip LD_{50} to about 10^3 fold (Table 1). Parallel line analysis of the regression lines was performed for each NTX on days 1, 2 and 4, followed by Tukey's test. The regression lines for all types of NTX showed parallelism, except for type C NTX (data not shown).

3.3. Inhibitory effect of the different NTX types on neuromuscular transmission

To compare the inhibition of neuromuscular transmission by the different types of NTX, the ED_{50} was defined as the dose that decreased the CMAP amplitude to 50% of the pre-toxin level, and was calculated for the peak effect at each dose. The ED_{50} rank order of NTX was type D > B > F > E > C > C/D > A. Type A NTX was most potent to reduce the CMAP amplitude, and type D NTX was lowest potent (Table 2).

3.4. Comparison of diffusion to the contralateral site and safety index of the different types of NTX

To compare diffusion to the contralateral site of the different types of NTX, the CMAP amplitude was measured in the right hind leg. The TD_{20} was defined as the dose that decreased the CMAP amplitude to 20% of the pre-toxin level and was calculated to assess the peak effect at each dose. The TD_{20} value rank order of NTX was type D > F > B > C > E > A > C/D. Type C/D NTX was most potent to diffuse to the contralateral site, and type D NTX the lowest potent. The ratio of TD_{20}/ED_{50} was calculated for each NTX, and is expressed as the safety index. The safety index rank order of NTX was type F > C > D > E > A > C/D > B. The results revealed that type F NTX showed the widest safety index and was hard to diffuse, and type B NTX the narrowest index and was prone to diffuse (Table 2).

3.5. Changes in CMAP amplitude induced by muscle relaxants (d-Tc and SCh)

To investigate whether the CMAP amplitude can accurately reflect the inhibition of neuromuscular transmission by botulinum toxin, we evaluated muscle relaxants with different mechanisms of action. The average CMAP amplitudes in groups treated with 0.01, 0.03, and 0.09 mg d-Tc were reduced to about 78, 15, and 2% of that in the vehicle group, whereas those in the groups treated with 0.1, 0.3, and 0.9 mg SCh were reduced to about 68, 12, and 1%, respectively. Differences were significant for both d-Tc and SCh ($p < 0.0001$; Jonckheere–Terpstra trend test). The muscle relaxants induced a dose-related decrease in the CMAP amplitude, similar to botulinum toxin, indicating that the CMAP test can be used to evaluate the inhibition of neuromuscular transmission.

3.6. Comparison of muscle flaccidity induced by the different types of NTX

To compare the muscle flaccidity-inducing effects of the different types of NTX, we evaluated them using the DAS assay. When the log of the ip LD_{50} and median DAS score were plotted on the horizontal and vertical axes, respectively, the reaction curves for each NTX showed dose-dependent linearity. The required toxin value rank order of NTX for muscle flaccidity was type B = D > F > E > A = C = C/D. Type A, C, and C/D NTX were most potent to exhibit a muscle flaccidity-inducing effect, and type B NTX was lowest potent (Fig. 3). The ip LD_{50} dose necessary to achieve a score of 1 in the DAS assay was greater than that required to reduce the CMAP amplitude.

4. Discussion

The neuromuscular transmission inhibitor (d-Tc and SCC) with different mechanisms of action to the botulinum toxin induced a dose-related decrease in the CMAP amplitude. This result indicated that the CMAP amplitude reflected the inhibition of neuromuscular transmission caused by the muscle flaccidly-inducing effect of the drug. The results generated by the CMAP test are continuous data, whereas those of the mouse ip LD_{50} method and scores are discrete data.

We used the rat CMAP test to determine the toxin activity of different NTX types. Type A and C/D NTX reduced the CMAP amplitude one day after administration at 0.01 and 0.03 ip LD_{50}, respectively. In contrast, 10 ip LD_{50} of type B NTX were needed to reduce the CMAP amplitude. Type A, C, C/D, and E NTX required a dose of 1 ip LD_{50} or below, and the CMAP method was more sensitive than the mouse ip

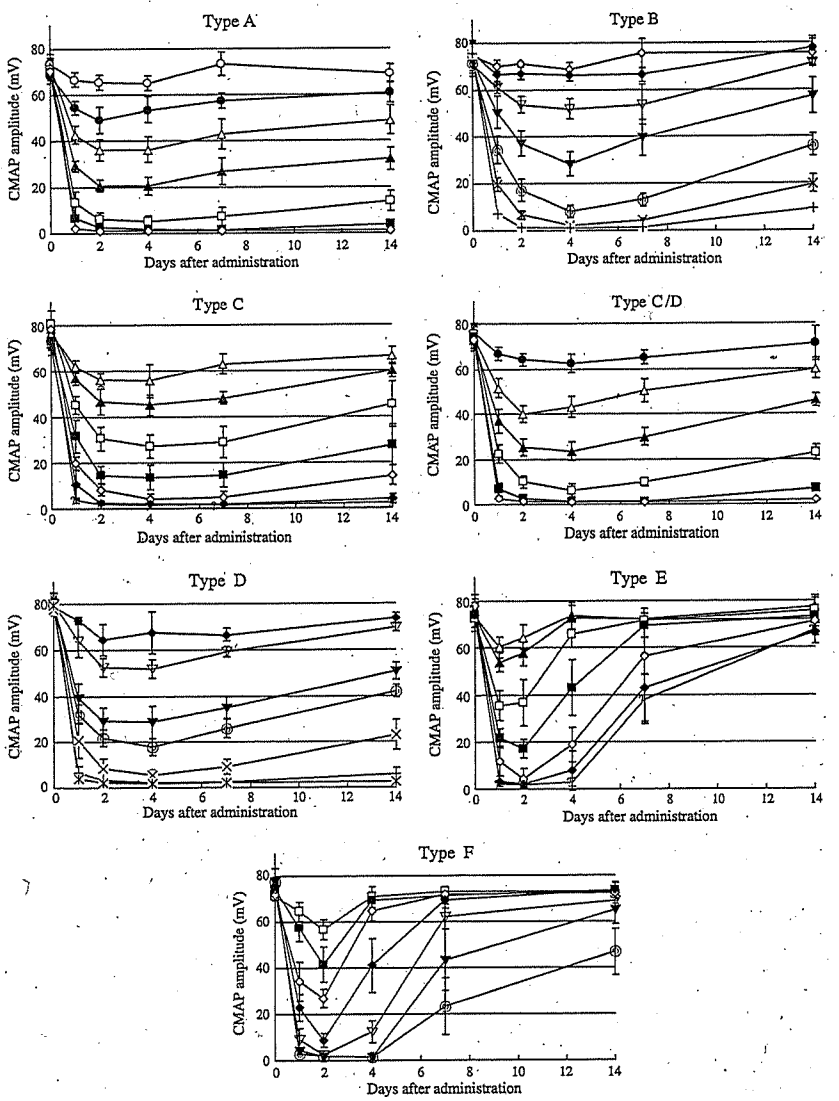

Fig. 1. Dose–response of the CMAP amplitude with the different NTX types at the injection site. Rats received botulinum toxin into left gastrocnemius muscle (○: 0.01 ip LD_{50}; ●: 0.03 ip LD_{50}; △: 0.1 ip LD_{50}; ▲: 0.3 ip LD_{50}; □: 1 ip LD_{50}; ■: 3 ip LD_{50}; ◇: 10 ip LD_{50}; ◆: 30 ip LD_{50}; ▽: 100 ip LD_{50}; ▼: 300 ip LD_{50}; ⊙: 1000 ip LD_{50}; ×: 3000 ip LD_{50}; +: 10,000 ip LD_{50} and •: 30,000 ip LD_{50}). CMAP amplitude was measured for the left hind leg of each rat at before and 1, 2, 4, 7, and 14 days after administration. Each point is the mean ± SD, $n = 5$.

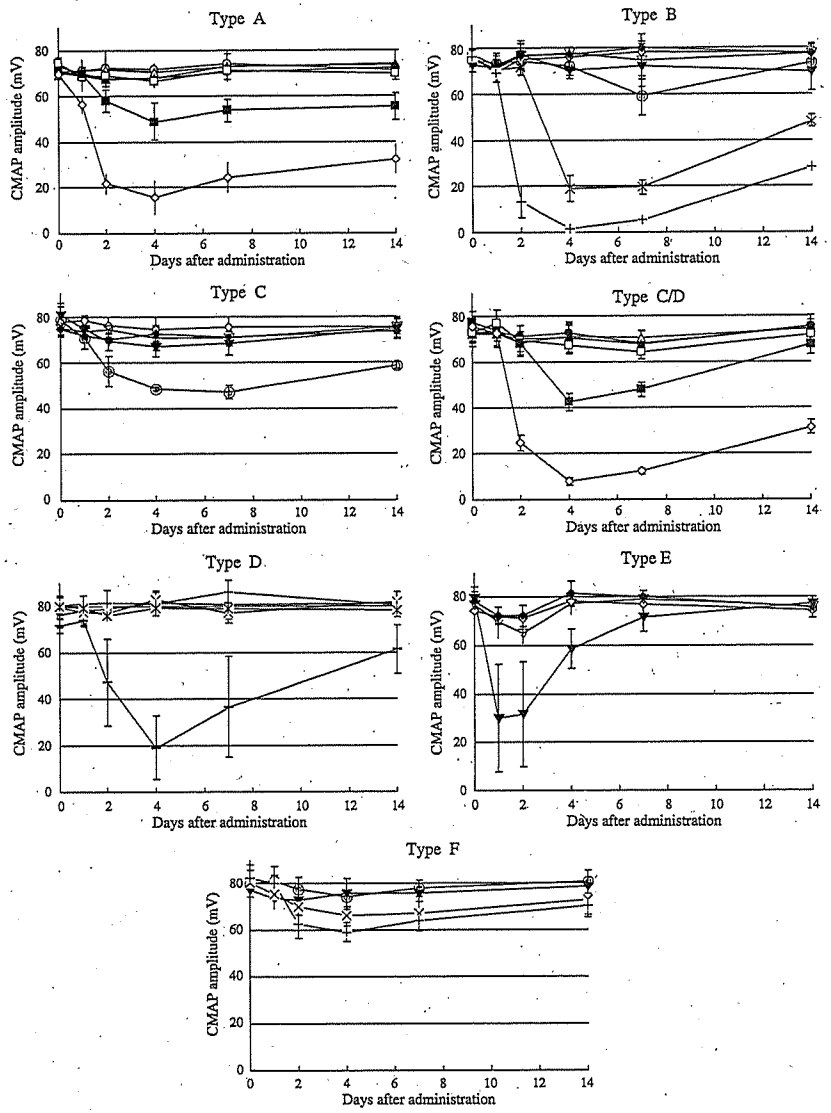

Fig. 2. Dose–response of the CMAP amplitude with the different NTX types at the contralateral site. Rats received botulinum toxin into left gastrocnemius muscle (○: 0.01 ip LD_{50}; ●: 0.03 ip LD_{50}; △: 0.1 ip LD_{50}; ▲: 0.3 ip LD_{50}; □: 1 ip LD_{50}; ■: 3 ip LD_{50}; ◇: 10 ip LD_{50}; ◆: 30 ip LD_{50}; ▽: 100 ip LD_{50}; ▼: 300 ip LD_{50}; ⊙: 1000 ip LD_{50}; ×: 3000 ip LD_{50}; +: 10,000 ip LD_{50}; •: 30,000 ip LD_{50} and –: 100,000 ip LD_{50}). CMAP amplitude was measured for the right hind leg of each rat at before and 1, 2, 4, 7, and 14 days after administration. Each point is the mean ± SD, $n = 5$.

Table 1
Linearity ranges on regression analysis of the CMAP amplitude after the administration of type A to F NTX.

Type	Linearity range (ip LD_{50})				
	1 day (R^2)[a]	2 day (R^2)	4 day (R^2)	7 day (R^2)	14 day (R^2)
A	0.01–30 (0.979)	0.01–10 (0.971)	0.01–10 (0.966)	0.01–10 (0.954)	0.01–10 (0.959)
B	10–10,000 (0.932)	10–10,000 (0.954)	10–10,000 (0.949)	10–10,000 (0.950)	10–10,000 (0.915)
C	0.1–100 (0.957)	0.1–30 (0.957)	0.1–30 (0.955)	0.1–30 (0.968)	0.1–100 (0.946)
C/D	0.03–10 (0.964)	0.03–10 (0.980)	0.03–3 (0.968)	0.03–3 (0.962)	0.03–10 (0.963)
D	30–30,000 (0.942)	30–30,000 (0.953)	30–10,000 (0.958)	30–10,000 (0.949)	30–30,000 (0.937)
E	0.1–30 (0.930)	0.1–30 (0.928)	0.3–100 (0.915)	–	–
F	1–300 (09.37)	1–300 (0.954)	10–300 (0.956)	–	–

[a] R^2: multiple correlation coefficient.

Table 2
ED_{50}, TD_{20}, and safety index values for type A to F NTX.

Type	ED_{50}[a] (ip LD_{50})	TD_{20}[b] (ip LD_{50})	Safety index (TD_{20}/ED_{50})
A	0.09	1.57	18
B	167	1226	7
C	0.54	385	718
C/D	0.13	1.38	11
D	206	36,433	177
E	0.85	50	59
F	4.67	3772	808

[a] ED_{50}, dose which caused a 50% reduction of the CMAP amplitude.
[b] TD_{20}, dose which caused a 20% reduction of the CMAP amplitude.

LD_{50} assay. However, in type B, D, and F NTX, the CMAP method was less sensitive. These results suggest that mice and rats show a different sensitivity to toxins. The results indicated an advantage whereby the method can be used to measure a broad range of toxin activities on the day following administration.

The rat CMAP test is useful not only for measuring toxin activity, but also for evaluating the characteristics of the neuromuscular transmission-inhibitory effect of different NTX types. To assess whether the neuromuscular transmission-inhibitory effect was correlated with the muscle flaccidity-inducing effect, the latter effect of the different NTX types was compared using the DAS assay. The neuromuscular transmission-inhibitory effect (ED_{50}) using the CMAP test was compared to that using the DAS assay, and all types of NTX showed a correlation between the effect of the inhibition of neuromuscular transmission and the potency of muscular flaccidly, except type C NTX. The ED_{50} of type C NTX showed a higher dose than that of type A and C/D NTX; however, the effect of flaccid muscle paralysis was the same. The toxins cleave SNARE proteins (i.e., SNAP-25, synaptobrevin, and syntaxin), which fuse to the synaptic vesicle and nerve cell membrane, blocking neuromuscular transmission by inhibiting the release of acetylcholine from synaptic vesicles. This suggested the possibility that the muscle-relaxing effect of type C NTX is caused not only by the inhibition of neuromuscular transmission through the cleavage of SNARE proteins, but also by other action mechanisms (i.e., the effect on the muscle).

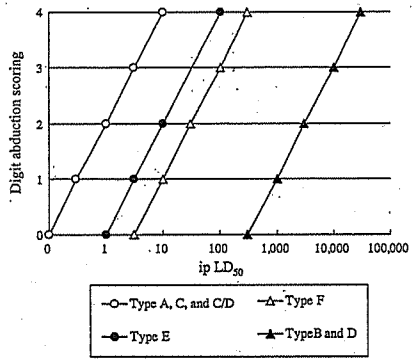

Fig. 3. Comparison of the muscle flaccidity-inducing effect of type A to F NTX on digit abduction in rats two days after administration. The scores indicate the median of each dose, $n = 5$.

Assuming that the findings can be extrapolated to humans, type A and C NTX might show a higher efficacy and safety than other types of NTX as muscle relaxants. Type A NTX showed the strongest effect on the inhibition of neuromuscular transmission and muscle flaccidity, having longer-lasting effects than type B NTX. Type A NTX showed a higher sensitivity than the other types of NTX in humans, and so might be the most suitable as a muscle relaxant. However, the results suggested that type A NTX has the disadvantage that it is prone to diffuse compared to the other types, except for type B and C/D NTX. Type C NTX might be the most suitable for relaxing a particular muscle, because it showed a potent muscle flaccidity-inducing effect and diffuses less than the other types. A dose inhalation toxicity study in monkeys showed equivalent effects between type A and C NTX (LeClaire and Pitt, 2005). In a clinical study, it was reported that type C had a muscle-relaxing effect equivalent to that of type A NTX (Eleopra et al., 1997; Eleopra et al. 2004).

Recently, type C, E, and F toxins have been tried as treatments for various diseases. The inhibitory effect of type E NTX on neuromuscular transmission was the fourth strongest after type A, C, and C/D NTX. The safety index of type E NTX was ranked fourth after type F, C, and D, and the duration of the effect of type E NTX was the shortest. It was reported that the muscular flaccidity-inducing effect of type E and F toxins was of a short duration in humans, similar to the result in this study. Since an effect of type E toxin on the central nervous system was reported (Bozzi et al., 2006), the toxin may be of use in diseases of the central nervous system. In the future, the other NTX except types A and B may be applied to treatment, and they might be approved as new drugs.

In this study, the rat CMAP test was able to quantify the toxin activity of types A–F toxin. This method is applicable to different types of botulinum toxin preparation which might be marketed, and aids in quality control. This method is useful for evaluating the pharmacological effects of muscle relaxants.

Acknowledgements

The present investigation was conducted with a part of financial support from the Society for the Japan Health Sciences Foundation.

Conflicts of interest

The authors declare that there are no conflicts of interest.

References

Aoki, K.R., 2001. A comparison of the safety margins of botulinum neurotoxin serotypes A, B, and F in mice. Toxicon 39 (12), 1815–1820.
Bigalke, H., Wohlfarth, K., Irmer, A., Dengler, R., 2001. Botulinum A toxin: Dysport improvement of biological availability. Exp. Neurol. 168 (1), 162–170.
Bozzi, Y., Costantin, L., Antonucci, F., Caleo, M., 2006. Action of botulinum neurotoxins in the central nervous system: antiepileptic effects. Neurotox. Res. 9 (2–3), 197–203.
Cichon Jr., J.V., McCaffrey, T.V., Litchy, W.J., Knops, J.L., 1995. The effect of botulinum toxin type A injection on compound muscle action potential in an in vivo rat model. Laryngoscope 105 (2), 144–148.
Eleopra, R., Tugnoli, V., Rossetto, O., Montecucco, C., De Grandis, D., 1997. Botulinum neurotoxin serotype C: a novel effective botulinum toxin therapy in human. Neurosci. Lett. 224 (2), 91–94.
Eleopra, R., Tugnoli, V., Rossetto, O., De Grandis, D., Montecucco, C., 1998. Different time course of recovery after poisoning with botulinum neurotoxin serotypes A and E in human. Neurosci. Lett. 256 (3), 135–138.
Eleopra, R., Tugnoli, V., Quatrale, R., Rossetto, O., Montecucco, C., 2004. Different types of botulinum toxin in humans. Mov. Disord. 19 (Suppl. 8), S53–S59.
Hallis, B., James, B.A., Shone, C.C., 1996. Development of novel assays for botulinum type A and B neurotoxins based on their endopeptidase activities. J. Clin. Microbiol. 34 (8), 1934–1938.
Jahn, R., Niemann, H., 1994. Molecular mechanisms of clostridial neurotoxins. Ann. N.Y. Acad. Sci. 733, 245–255.
Jankovic, J., 2004. Botulinum toxin in clinical practice. J. Neurol. Neurosurg. Psychiatr. 75 (7), 951–957.
Kessler, K.R., Benecke, R., 1997. The EDB test – a clinical test for the detection of antibodies to botulinum toxin type A. Mov. Disord. 12 (1), 95–99.
LeClaire, R.D., Pitt, M., 2005. Biological weapons defense. In: Lindler, L.E., Lebeda, F.J., Korch, G.W. (Eds.), Biological Weapon Defense: Infectious Diseases and Counterbioterrorism. Humana Press, Totowa, pp. 41–61.
Mezaki, T., Kaji, R., Kohara, N., Fujii, H., Katayama, M., Shimizu, T., Kimura, J., Brin, M.F., 1995. Comparison of therapeutic efficacies of type A and F botulinum toxins for blepharospasm: a double-blind, controlled study. Neurology 45 (3 Pt 1), 506–508.
Montecucco, C., Schiavo, G., 1994. Mechanism of action of tetanus and botulinum neurotoxins. Mol. Mirobiol. 13 (1), 1–8.
Pearce, L.B., Borodic, G.E., First, E.R., MacCallum, R.D., 1994. Measurement of botulinum toxin activity: evaluation of the lethality assay. Toxicol. Appl. Pharmacol. 128 (1), 69–77.
Sakaguchi, G., Ohishi, I., Kozaki, S., 1981. Purification and oral toxicities of *Clostridium botulinum* progenitor toxins. In: Lewis, G.E. (Ed.), Biomedical Aspect of Botulism. Academic Press, New York, pp. 21–34.
Sakaguchi, G., 1983. *Clostridium botulinum* toxins. Pharmacol. Ther. 19 (2), 165–194.
Schiavo, G., Matteoli, M., Montecucco, C., 2000. Neurotoxins affecting neuroexocytosis. Physiol. Rev. 80 (2), 717–766.
Sesardic, D., McLellan, K., Ekong, T.A., Das, R.G., 1996. Refinement and validation of an alternative bioassay for potency testing of therapeutic botulinum type A toxin. Pharmacol. Toxicol. 78 (5), 283–288.
Straughan, D., 2006. Progress in applying the three Rs to the potency testing of botulinum toxin type A. Altern. Lab. Anim. 34 (3), 305–313.
Takahashi, M., Kameyama, S., Sakaguchi, G., 1990. Assay in mice for low levels of *Clostridium botulinum* toxin. Int. J. Food Microbiol. 11 (3–4), 271–277.
Wictome, M., Newton, K., Jameson, K., Hallis, B., Dunnigan, P., Mackay, E., Clarke, S., Taylor, R., Gaze, J., Foster, K., Shone, C., 1999. Development of an in vitro bioassay for *Clostridium botulinum* type B neurotoxin in foods that is more sensitive than the mouse bioassay. Appl. Environ. Microbiol. 65 (9), 3787–3792.
Yoneda, S., Shimazawa, M., Kato, M., Nonoyama, A., Torii, Y., Nishino, H., Sugimoto, N., Kozaki, S., Hara, H., 2005. Comparison of the therapeutic indexes of different molecular forms of botulinum toxin type A. Eur. J. Pharmacol. 508 (1–3), 223–229.

Toxicon 54 (2009) 857–861

Contents lists available at ScienceDirect

Toxicon

journal homepage: www.elsevier.com/locate/toxicon

Quantitative determination of the biological activity of botulinum toxin type A by measuring the compound muscle action potential (CMAP) in rats

Takashi Sakamoto [a], Yasushi Torii [b,c,*], Motohide Takahashi [d], Setsuji Ishida [d], Yoshitaka Goto [b], Hirotoshi Nakano [b], Tetsuhiro Harakawa [b], Akihiro Ginnaga [b], Shunji Kozaki [c], Ryuji Kaji [e]

[a] Department of Neurology, National Center Hospital of Neurology and Psychiatry, 4-1-1 Ogawa-Higashi, Kodaira-shi, Tokyo 187-8551, Japan
[b] The Chemo-Sero-Therapeutic Research Institute (KAKETSUKEN), 1-6-1 Okubo, Kumamoto-shi, Kumamoto 860-8568, Japan
[c] Department of Veterinary Sciences, School of Life and Environmental Sciences, Osaka Prefecture University, 1-18 Rinku-oraikita, Izumisano-shi, Osaka 599-8531, Japan
[d] Department of Bacterial Pathogenesis and Infection Control, National Institute of Infectious Diseases, 4-7-1 Gakuen, Musashimurayama-shi, Tokyo 208-0011, Japan
[e] School of Medicine, University of Tokushima Faculty of Medicine, 18-15 Kuramoto-cho, Tokushima-shi, Tokushima 770-8503, Japan

ARTICLE INFO

Article history:
Received 9 February 2009
Received in revised form 12 June 2009
Accepted 16 June 2009
Available online 25 June 2009

Keywords:
Clostridium botulinum
CMAP
Mouse ip LD_{50}

ABSTRACT

Quantitative determination of the biological activity of botulinum toxin type A usually depends on the LD_{50} method after intraperitoneal injection into mice. This method requires a large number of mice to determine the toxic activity at a high level of precision and 3–4 days to obtain the results. Techniques to replace the LD_{50} method have been attempted at various institutes. As a substitute for this method, by directly measuring the inhibition of neuromuscular transmission after the administration of a toxin, a method to quantitatively assess the toxin's activity by determining the compound muscle action potential (CMAP) was examined. Toxin solutions were injected into the rat gastrocnemius muscle, and that of the CMAP amplitude was determined over time. The CMAP amplitude decreased over 4 days after the injection of the toxin, and then slowly recovered. A dose-response relationship was noted for each dose, and a linear relation was observed between 0.01 and 30 U on the 1st day. From these results, we propose the CMAP as a substitute for the LD_{50} method to examine the activity of toxin products as it is simple and reliable, reduces the number of experimental animals required, and lowers pain levels.

1. Introduction

Clostridium botulinum produces toxins that have been classified into 7 serotypes, A, B, C, D, E, F, and G, based on their immunological characteristics. The toxins act on neuromuscular junctions and induce muscle relaxation by inhibiting acetylcholine release (Sakaguchi, 1983). Type A and B toxin preparations have been utilized as a treatment for spasm in myotonus and dystonia (Jankovic, 2004; Sadick, 2003).

The standard method to determine the biological activity of botulinum toxin is the lethal dose 50% (LD_{50}) test involving intraperitoneal (ip) injection into mice, and many mice are required to ensure sufficient accuracy levels for the quality control of preparations, which has posed a problem with regard to animal welfare (Pearce et al., 1994). International meetings on alternative methods for animal testing have been held, and replacements for the mouse ip LD_{50} test have been discussed (Straughan, 2006).

* Corresponding author at: Human Vaccine Production Department, the Chemo-Sero-Therapeutic Research Institute (KAKETSUKEN), 1-6-1 Okubo, Kumamoto-shi, Kumamoto 860-8568, Japan. Tel.: +81 96 344 1211; fax: +81 96 345 1345.
E-mail address: torii-ya@kaketsuken.or.jp (Y. Torii).

0041-0101/$ – see front matter © 2009 Elsevier Ltd. All rights reserved.
doi:10.1016/j.toxicon.2009.06.020

The 3 Rs (refinement, reduction, and replacement) have been proposed for alterative methods, and alternative *in-vitro*, *ex-vivo*, and *in-vivo* test systems have been investigated. The *in-vitro* test system, ELISA, determining the endopeptidase activity, does not use animals, but the sensitivity is lower than the mouse bioassay (Hallis et al., 1996; Wictome et al., 1999). This method could determine only light-chain activity in many cases, and the inaccurate determination of toxin function has been reported. The *ex-vivo* test system using the mouse phrenic nerve-hemidiaphragm is sensitive, but it requires skilled techniques, and has a low reproducibility (Yoneda et al., 2005; Bigalke et al., 2001). The *in-vivo* test systems, such as the digit abduction scoring (DAS) assay and local flaccid paralysis assay, use scores for evaluation (Aoki, 2001; Takahashi et al., 1990; Sesardic et al., 1996). When an evaluation lies between two scores, judgment is difficult. As each test system has both advantages and disadvantages, no alternative method has been established.

We attached a greater importance to the following point in devising an alternative method to determine the activity of botulinum toxin: the potency of botulinum toxin preparations should be evaluated based on their pharmacological effect of inhibiting neuromuscular transmission, and not based on their lethal activity, as in the mouse ip LD_{50} assay. There are several test systems to evaluate the inhibition of neuromuscular transmission, and we focused on the measurement of the compound muscle action potential (CMAP) used for the diagnosis of various nervous disorders. The CMAP is generated by the contraction of muscle fibers; the microcurrent generated by muscle contraction is amplified and recorded. Botulinum toxin affects nerve endings to suppress neurotransmission. Therefore, by determining the CMAP amplitude, the action of the toxin suppressing the transmission of electric stimulation to the muscle can be shown numerically. CMAP measurement is utilized by the extensor digitorum brevis (EDB) test, which checks the response to the toxin before treatment in patients who might have antibodies to the botulinum toxin (Kessler and Benecke, 1997). It was reported that the CMAP amplitude was measured in the rat gastrocnemius muscle which was injected several times with botulinum toxin (Cichon et al., 1995). The CMAP amplitude decreased as the toxin activity increased, but quantitative determination of the toxin was not carried out. Based on this previous CMAP study, we investigated a botulinum toxin quantification method, aiming at replacing the mouse ip LD_{50} assay.

2. Materials and methods

2.1. Toxin preparation

Botulinum neurotoxin type A (150 kDa, NTX) was prepared using modified culture and purification methods, as previously reported (Sakaguchi et al., 1981). *C. botulinum* type A strain A2 was cultured in PYG medium containing 2% peptone, 0.5% yeast extract, 0.5% glucose, and 0.025% sodium thioglycolate in a glass bottle. After incubation for 3 days at 30 °C, the culture fluid was adjusted to pH 3.5 by adding 1.5 M sulfuric acid. The precipitate was collected by centrifugation, and the crude toxin was extracted with 0.2 M phosphate buffer (pH 6.0). The extract contained nucleic acids, which were removed by treating with 2% protamine sulfate, and the precipitate was removed by centrifugation. The supernatant was precipitated at a 60% saturation of ammonium sulfate, and the precipitate, collected by centrifugation, was dialyzed against 0.05 M acetate buffer containing 0.2 M sodium chloride (pH 4.2). The dialyzed material was applied to an SP-Sephadex column equilibrated with the same buffer. Then, M toxin was eluted using a linear gradient of sodium chloride concentrations from 0.2 to 0.7 M. M toxin was dialyzed against 10 mM phosphate buffer (pH 7.5), adsorbed onto a DEAE sepharose column equilibrated with the same buffer, and eluted with a 0–0.3 M NaCl gradient in the buffer to separate NTX and nontoxic proteins. The NTX was concentrated to 1 mg/mL using the YM-10 membrane (Millipore, Tokyo, Japan), dialyzed against 10 mM phosphate buffer (pH 7.5), and stored at −70 °C until use.

For the test control, commercial progenitor LL toxin (900 kDa, BOTOX®, Allergan Inc., U.S., LL hereafter) was used.

2.2. Experimental animals

Female ICR/CD-1 mice (4 weeks of age, about 20 g) for the LD_{50} test and female S/D rats (8 weeks of age, about 200 g) for the CMAP test were purchased from Charles River Laboratories Japan (Tokyo, Japan). The animal room was maintained under controlled light/dark conditions, and animals were given free access to feed and water. This study was performed in accordance with the guidelines concerning experimental animals established by the Japanese Pharmacological Society, and approved by the Internal Animal Ethics Committee.

2.3. Mouse ip LD_{50} assay

The toxin activity of NTX and LL was determined by the mouse intraperitoneal LD_{50} method, defining one mouse ip LD_{50} = 1 unit (U) (Pearce et al., 1994). The mouse ip LD_{50} was determined by employing an assay involving 7 doses at a dilution interval of 1.25 and 20 animals per dose. The chosen evaluation period was the first 96 h after administration, and the LD_{50} was calculated using the probit method.

2.4. Toxin administration

Each toxin was serially diluted with physiological saline containing 0.5 w/v% human serum albumin, and 0.1–300 U/mL solutions were prepared. Rats were anesthetized by an intraperitoneal injection of about 40 mg/kg pentobarbital sodium (Kyoritsu Seiyaku, Tokyo, Japan). After the eyelid reflex had disappeared, the hind leg was shaved, and 0.1 mL of the toxin dilution was injected into the left hind gastrocnemius muscle using a 30-G insulin syringe (Becton Dickinson, Tokyo, Japan).

2.5. CMAP measurement

The CMAP was measured using Nicolet Viking Quest (Viasys Healthcare, Tokyo, Japan). Rats were anaesthetized and fixed in the prone position. The electrode used was an alligator clip lead wire (Viasys Healthcare, Tokyo, Japan),

attached to the skin. The electrode attachment sites are shown in Fig. 1. The stimulating electrode (cathode) was placed on the skin over the fourth lumbar vertebra. The stimulating electrode (anode) was placed at 2 cm from the cathode on the spinal column. The recording electrode was placed on the belly muscle of the left hind gastrocnemius muscle, the reference recording electrode on the left hind gastrocnemius tendon, and the earth electrode on the tail root. Electric stimulation was loaded at 25 mA for 0.2 ms, and the CMAP was obtained. The CMAP was measured before (0) and 1, 2, 4, 7, and 14 days after administration.

2.6. Statistical analysis

For analysis of the CMAP amplitude, Statistical Analysis for Neurotoxin (SAN, ver. 1.05) was used. The waveform of one CMAP was converted to 2000 dots using the software supplied with the electromyograph, and the coordinates of the dots were converted to numbers. The distance between the top and bottom of the waveform was calculated using SAN as the CMAP amplitude. SAN was created to store raw data of the CMAP amplitude and perform various statistical analyses (*t*-test, one-way and two-way layout ANOVA, regression analysis, parallel line analysis, and correlation coefficient).

For the confirmation of CMAP quantifiability, logarithm LD_{50} doses on horizontal and logit-transformed CMAP amplitudes on vertical axes were plotted, respectively, and the linearity of the regression line was confirmed by regression analysis.

3. Results

3.1. Toxin activity

The toxin activity of NTX and LL was 93,000 ± 565 U and 92.4 ± 1.48 U, respectively.

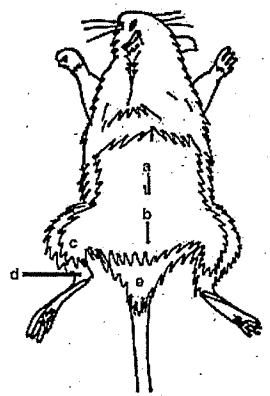

Fig. 1. CMAP measurement method. a. Stimulating electrode (+); b. Stimulating electrode (−); c. Recording electrode (−) and injection site; d. Recording electrode (+); e. Grounding electrode.

3.2. Dose-responsiveness of the CMAP

On time-course measurement of the CMAP amplitude after NTX administration, the left hind leg CMAP amplitude decreased until the 4th day, and then slowly recovered after the 7th day. Limb paralysis was observed after the administration of 3 U or more. It was found that the CMAP amplitude decreased depending on the concentration of LD_{50} doses (Fig. 2). These results were subjected to regression analysis, and linearity was detected over a range of 0.01–30 U on day 1 ($R^2 = 0.979$) (Fig. 3), and 0.01–10 U on days 2, 4, 7, and 14 ($R^2 = 0.971$ on day 2, $R^2 = 0.966$ on day 4, $R^2 = 0.954$ on day 7, and $R^2 = 0.959$ on day 14, respectively).

To investigate whether other molecular forms of the toxin show a different dose-responsiveness regarding NTX, the CMAP amplitude was measured in the same experiment using LL, and the linearity of the regression line between the CMAP amplitude and potency was verified. Parallel line analysis of the regression lines of NTX and LL on the 1st day after administration indicated that the regression lines of toxins were parallel to each other. No significant difference was noted between the two lines, and the relative potency of LL in relation to NTX was 0.965 (95% confidence interval: 0.791–1.178). Accordingly, the same calibration curve could be used for the evaluation of type A preparations, NTX and LL (Fig. 3).

3.3. Reproducibility of the CMAP test

Reliability is important for substance-measurement methods, and reproducibility is essential. To confirm the reproducibility, the CMAP amplitude was measured 3 times using the same procedure on different days and by two measurers. The reactions after administration were similar. The regression lines of the dose-response curve of NTX and LL on the 1st day after administration were analyzed by two measurers, and were parallel to each other. The relative potency of LL as assessed by the two measurers was 0.958 (95% confidence interval: 0.763–1.203), showing that there was no significant difference in the dose-response regression lines for LL obtained by them (data not shown). This result suggested that the CMAP test regarding the response to toxin activity was reproducible.

3.4. Time-course CMAP amplitude of botulinum toxin-treated muscle

We investigated whether time-course reactions of the CMAP amplitude could be fitted to an equation, and found that the amplitude after administration conformed to the following experimental equation: $y = a - b(\log(x)) + C(\log(x)\log(x))$ (the equation represents a physical phenomenon). Using this equation, the days showing a maximum reduction of the CMAP amplitude, recovery to the pre-treatment condition, 50% recovery, and 50% amplitude reduction can be calculated. For example, the days after the administration of 0.1 U NTX shown in Table 1 were predicted using this equation.

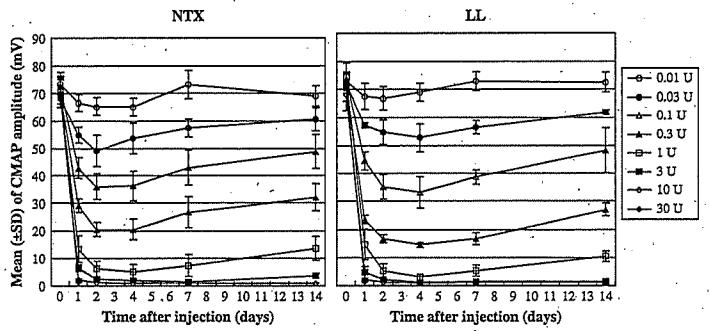

Fig. 2. Dose-response of the CMAP amplitude of NTX and LL. Each point is the mean ± SD ($n = 5$).

4. Discussion

The mouse ip LD_{50} method, a quantitative method for determining the biological activity of botulinum toxin now widely used, is based on lethality in mice, but the method requires 3–4 days to make a judgment and many animals to obtain reliable results. Various alternative methods have been investigated for the quantification of botulinum toxin, but all have advantages and disadvantages, and so an appropriate replacement test is still awaited.

We investigated the possibility of using the rat CMAP test as a substitute for the mouse ip LD_{50} assay, and identified a dose-response relationship with the mouse ip LD_{50} dose (toxin activity) at 1, 2, 4, 7, and 14 days after injection and the capability of measuring the duration of the toxin's effect. This method was very sensitive, facilitating measurement down to a sensitivity of 0.01 U, which is not possible using the mouse ip LD_{50} assay, and a regression line within a broad range of 0.01–30 U was obtained 1 day after administration. The toxin activity could be measured

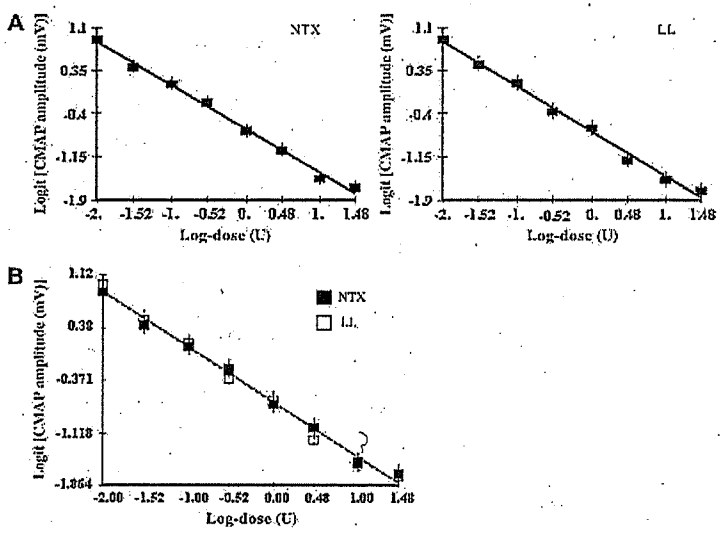

Fig. 3. Regression analysis of the CMAP amplitude of NTX and LL on the 1st day after administration (A), and parallel line analysis of the regression line of NTX and LL on the 1st day after administration (B). Each point is the mean ± 95% confidence interval ($n = 5$).

Table 1
Days after administration of 0.1 U NTX predicted from the response curve.

	Day
Day showing maximum reduction	4.7
Day showing recovery to pre-treatment condition	32.0
Day showing 50% recovery	13.3
Day showing 50% amplitude reduction	1.3

on the day following administration, which is a major advantage. In addition, the number of experimental animals required can be markedly reduced because of the broad range and its high-level precision. Furthermore, the results obtained by the LD_{50} method and score represent a discrete quantity, while those generated by the CMAP test represent a continuous quantity. Thus, statistical processing is applicable, and the quantity of information obtainable is large.

Analysis using SAN clarified that the time-course reactions of the CMAP amplitude fitted an equation. By applying this equation, the CMAP method may be used for not only quantification of the toxin but also the evaluation of its various pharmacological effects. Time-course changes in the amplitude can be predicted by substituting several measurement data in the equation. For example, the duration of an effect of the toxin can be measured with data at minimum measurement points, which may reduce the number of experimental animals needed.

Results determined by several operators or on different days showed satisfactory intermediate-level precision, suggesting that the method is very suitable for the comparison of several toxin preparations and quality control. The difference in the muscle-relaxing effect between equal units of BOTOX® and Dysport® has been problematic in clinical practice (Rosales et al., 2006). To overcome this problem, whether an international standard for the toxin could be established was discussed, and investigated using the mouse ip LD_{50} assay at several laboratories. However, the possibility of its establishment is questionable because the results showed large variation. It was also investigated using other test methods, but the outcome was the same. As each test system has both advantages and disadvantages, no system for evaluating toxin function is both easy to perform and highly reproducible. On the other hand, the rat CMAP test is easy to conduct, highly reproducible, and can directly determine the effects of toxin preparations by assessing the inhibition of neuromuscular transmission. Thus, it is suitable for the quality control and evaluation of toxin preparations. The rat CMAP test is also cheaper to conduct than the mouse ip LD_{50} test.

We propose that the CMAP test with the characteristics described above is an alternative method for the quantification of botulinum toxin.

Acknowledgment

The present investigation was conducted with financial support from the Society for the Japan Health Sciences Foundation.

Conflict of interest

The authors declare that there are no conflicts of interest.

References

Aoki, K.R., 2001. A comparison of the safety margins of botulinum neurotoxin serotypes A, B, and F in mice. Toxicon 39 (12), 1815–1820.
Bigalke, H., Wohlfarth, K., Irmer, A., Dengler, R., 2001. Botulinum A toxin: Dysport improvement of biological availability. Exp. Neurol. 168 (1), 162–170.
Cichon Jr., J.V., McCaffrey, T.V., Litchy, W.J., Knops, J.L., 1995. The effect of botulinum toxin type A injection on compound muscle action potential in an in vivo rat model. Laryngoscope 105 (2), 144–148.
Hallis, B., James, B.A., Shone, C.C., 1996. Development of novel assays for botulinum type A and B neurotoxins based on their endopeptidase activities. J. Clin. Microbiol. 34 (8), 1934–1938.
Jankovic, J., 2004. Botulinum toxin in clinical practice. J. Neurol. Neurosurg. Psychiatry 75 (7), 951–957.
Kessler, K.R., Benecke, R., 1997. The EDB test – a clinical test for the detection of antibodies to botulinum toxin type A. Mov. Disord. 12 (1), 95–99.
Pearce, L.B., Borodic, G.E., First, E.R., MacCallum, R.D., 1994. Measurement of botulinum toxin activity: evaluation of the lethality assay. Toxicol. Appl. Pharmacol. 128 (1), 69–77.
Rosales, R.L., Bigalke, H., Dressler, D., 2006. Pharmacology of botulinum toxin: differences between type A preparations. Eur. J. Neurol. 13 (Suppl. 1), 2–10.
Sadick, N.S., 2003. Botulinum toxin type B. Dermatol. Surg. 29 (4), 348–351.
Sakaguchi, G., Ohishi, I., Kozaki, S., 1981. Purification and oral toxicities of *Clostridium botulinum* progenitor toxins. In: Lewis, G.E. (Ed.), Biomedical Aspects of Botulism. Academic Press, New York, pp. 21–34.
Sakaguchi, G., 1983. *Clostridium botulinum* toxins. Pharmacol. Ther. 19 (2), 165–194.
Sesardic, D., McLellan, K., Ekong, T.A., Das, R.G., 1996. Refinement and validation of an alternative bioassay for potency testing of therapeutic botulinum type A toxin. Pharmacol. Toxicol. 78 (5), 283–288.
Straughan, D., 2006. Progress in applying the three Rs to the potency testing of botulinum toxin type A. Altern. Lab Anim. 34 (3), 305–313.
Takahashi, M., Kameyama, S., Sakaguchi, G., 1990. Assay in mice for low levels of *Clostridium botulinum* toxin. Int. J. Food Microbiol. 11 (3–4), 271–277.
Wictome, M., Newton, K., Jameson, K., Hallis, B., Dunnigan, P., Mackay, E., Clarke, S., Taylor, R., Gaze, J., Foster, K., Shone, C., 1999. Development of an in vitro bioassay for *Clostridium botulinum* type B neurotoxin in foods that is more sensitive than the mouse bioassay. Appl. Environ. Microbiol. 65 (9), 3787–3792.
Yoneda, S., Shimazawa, M., Kato, M., Nonoyama, A., Torii, Y., Nishino, H., Sugimoto, N., Kozaki, S., Hara, H., 2005. Comparison of the therapeutic indexes of different molecular forms of botulinum toxin type A. Eur. J. Pharmacol. 508 (1–3), 223–229.

Contents lists available at ScienceDirect

Toxicon

journal homepage: www.elsevier.com/locate/toxicon

Short communication

Quantification of potency of neutralizing antibodies to botulinum toxin using compound muscle action potential (CMAP)

Yasushi Torii [a,b,*], Motohide Takahashi [c], Setsuji Ishida [c], Yoshitaka Goto [a], Shinji Nakahira [a], Tetsuhiro Harakawa [a], Ryuji Kaji [d], Shunji Kozaki [b], Akihiro Ginnaga [a]

[a] The Chemo-Sero-Therapeutic Research Institute (KAKETSUKEN), 1-6-1 Okubo, Kumamoto-shi, Kumamoto 860-8568, Japan
[b] Department of Veterinary Sciences, School of Life and Environmental Sciences, Osaka Prefecture University, 1-18 Rinku-oraikita, Izumisano-shi, Osaka 598-8531, Japan
[c] Department of Bacterial Pathogenesis and Infection Control, National Institute of Infectious Diseases, 4-7-1 Gakuen, Musashimurayama-shi, Tokyo 208-0011, Japan
[d] School of Medicine, The University of Tokushima Faculty of Medicine, 18-15 Kuramoto-cho, Tokushima-shi, Tokushima 770-8503, Japan

ARTICLE INFO

Article history:
Received 24 June 2009
Received in revised form
13 September 2009
Accepted 15 September 2009
Available online 22 September 2009

Keywords:
Botulinum toxin
CMAP
Mouse neutralization test
ELISA

ABSTRACT

We evaluated a method for quantifying botulinum toxin-neutralizing antibodies which utilizes the CMAP. This method can be used just one day after administration, and the detection sensitivity was higher than that of the mouse neutralization test. The CMAP neutralization test detected neutralizing antibodies in patients who were resistant to treatment with the botulinum LL toxin. These results indicate that the CMAP neutralization test is useful for detecting low levels of antitoxin.

Botulinum toxins have recently been developed and used in the treatment of blepharospasm, spasmodic torticollis, dystonia, pain, and urological disorders (Jankovic, 2004; Truong and Jost, 2006; Casale and Tugnoli, 2008). The toxins show a high-level efficacy at very low doses, and are widely used in medical treatment. Resistance to the toxin was reported in some patients who received repeat high-dose (>100 mouse ip LD_{50} per injection cycle) toxin therapy over a long period of time (Borodic et al., 1996; Sesardic et al., 2004; Dressler, 2004). This reduced therapeutic response was reported to lead to the development of neutralizing antibodies in the patients. The potency of neutralizing antibodies in the serum of patients is measured using the mouse neutralization test (Hatheway et al., 1984). This method is based on the LD_{50} assay, which, in turn, is based on the number of surviving mice typically 96 h after the intraperitoneal (ip) injection of a fixed lethal dose of toxin premixed with different amounts of antitoxin. The antitoxin titer in the sample is expressed relative to that of the standard botulinum antitoxin. The detection limit of this method is reported to be about 10–100 mU/mL (Sesardic et al., 2004; Byrne et al., 1998). A reduced therapeutic response in certain patients was reported to be caused by minute amounts of antibodies which could not be detected by the mouse neutralization test (Sesardic et al., 2004). To detect neutralizing antibody presence in patients, a highly sensitive assay for neutralizing antibodies is needed. We reported quantitative of biological activity of botulinum toxin using the compound muscle action potential (CMAP) (Torii et al., submitted for publication). CMAP measurement is utilized by the extensor digitorum brevis (EDB) test, which qualitatively assesses the response to the toxin before treatment in patients who might possess antibodies against the botulinum toxin (Kessler and Benecke, 1997). Based on the EDB test, we investigated a highly sensitive quantification method for botulinum toxin-neutralizing antibodies in animal and human sera. In addition, we investigated whether the CMAP neutralization test was able to detect antitoxin in patient's serum, and we compared detection capability of this method, mouse neutralization test and ELISA.

Botulinum neurotoxin types A, B, E, and F (150 kDa, NTX) were cultured and purified using a previously reported method (Sakaguchi et al., 1981; Torii et al., submitted for publication). Equine-derived Japanese standard botulinum antitoxin types A, B, E, and F (National Institute of Infectious Diseases, Tokyo, Japan) were each used as a standard. One unit (U) of corresponding type of standard botulinum antitoxin neutralizes 10,000 mouse intraperitoneally (ip) LD_{50} of toxin types A, B, F or 1000 mouse ip LD_{50} of toxin type E (Jones et al., 2006). The sera of seven patients resistant to treatment with the botulinum LL toxin (BOTOX®, Allergan, Irvine, U.S.) were collected after informed consent was obtained. For the negative control, sera were collected from one volunteer who did not receive any treatment of botulinum toxin. For the positive control, sera were collected from one volunteer who had been immunized three times with the botulinum tetravalent (A, B, E, and F) toxoid. CMAP neutralization test was performed using a modification of a previously report method of CMAP test using female S/D rats (8 weeks of age, Charles River Laboratories Japan, Yokohama, Japan) (Torii et al., submitted for publication). Modification was using mixture which botulinum antitoxins and test toxins in place of toxins. Mixtures were prepared as follows: the standard botulinum antitoxin and various sera were serially diluted with physiological saline containing 0.5% human serum albumin. The test toxins comprised NTX of each type, at quantities whereby the CMAP amplitudes on day 1 after injection were decreased to one quarter of those before administration (type A: 10 mouse ip LD_{50}/mL, B: 60,000 mouse ip LD_{50}/mL, E: 60 mouse ip LD_{50}/mL, F: 600 mouse ip LD_{50}/mL). The type A of test toxin dose also was set at 1 mouse ip LD_{50}/mL to increase the measurement sensitivity. Equal volumes of the antitoxin or serum and test toxin were mixed and reacted for 1 h at room temperature. The anesthetized rats were injected 0.1 mL of a mixture into the left gastrocnemius muscle. The CMAP amplitude of the left hind leg was measured before (0) and 24 h after injection. The mouse neutralization test was performed using a previously reported method using female ICR/CD-1 mice (4 weeks of age, Charles River Laboratories Japan, Yokohama, Japan) (Torii et al., 2002). ELISA was performed using a modification of a previously reported method (Torii et al., 2002). Modifications were buffer using Tris Buffer containing 0.15 M NaCl, secondary antibody using peroxidase-conjugated goat anti-human IgG, IgA and IgM (Sigma, Tokyo, Japan) and substrate using TMB Microwell Peroxidase Substrate (Kirkegaard and Perry Laboratories Inc, Gaithersburg, U.S.). ELISA titers were expressed in multiples of absorbance of the negative control, and antibodies were considered to be detected by ELISA when the absorbance of the sample was more than twice that of the negative control. To determine whether the neutralizing antibody of each type was quantifiable, antibody potencies were plotted versus CMAP amplitudes, and the linearity of the regression line was confirmed by regression analysis using Statistical Analysis for Neurotoxin (SAN, ver. 2.1, self made soft). To determine the antibody titers of patients' sera, the amplitude data of standard botulinum antitoxin were calculated by regression analysis, and the regression line was used as the calibration curve using SAN.

The CMAP amplitude of each mixture of antitoxin and test toxin (types A, B, E, and F) decreased along with the antitoxin titer. For types A and E, regression analysis was performed by plotting the logarithmic values of the CMAP amplitude and antitoxin titer on the vertical and horizontal axes, respectively, and linearity was noted within a range of 3–100 mU/mL in type A ($R^2 = 0.983$) and 1–50 mU/mL in type E ($R^2 = 0.989$). For types B and F, the CMAP amplitudes were plotted on the vertical axis, and the log values of the antitoxin titer on the horizontal axis, and linearity was noted within a range of 25–100 mU/mL in type B ($R^2 = 0.953$) and 3–50 mU/mL in type F ($R^2 = 0.974$) (Fig. 1). To increase the measurement sensitivity, the test toxin dose was set at 1 mouse ip LD_{50}/mL in type A, and linearity was noted within a range of 1–6 mU/mL (data not shown). This method can be used to measure a broad range of neutralizing antibodies titers the day after administration. In this study, the CMAP neutralization test demonstrated six advantages over the standard technique. 1) The CMAP is more sensitive than the mouse neutralization test. 2) The CMAP neutralization test incorporates a concise procedure. 3) The CMAP neutralization test can determine the neutralizing antibody titer within 24 h; whereas, the mouse neutralization test requires 4 days to obtain the same results. 4) The CMAP neutralization test is highly reproducible. 5) Only 20–30 animals are used in the CMAP neutralization test, whereas more than 100 animals are necessary in a single mouse neutralization test. In addition, the rats are anesthetized during the test, and the amounts of injected test toxin do not completely block neuromuscular transmission nor paralyze the muscles. 6) The CMAP amplitude values obtained by the CMAP neutralization test are a continuous quantity. Taken together, these advantages indicate that this method is a useful substitute for the mouse neutralization test.

We then investigated whether minute amounts of neutralizing antitoxin present in patients' sera could be detected by the CMAP neutralization test. The neutralization antibodies in seven patients who showed a reduced therapeutic effect after repeated treatment with type A botulinum LL toxin were determined by the CMAP neutralization test, mouse neutralization test, and ELISA. Using the CMAP neutralization test, all sera showed a neutralizing antibody level of 3–50 mU/mL (Table 1). This suggests that the cause of the reduced therapeutic effect was the production of neutralizing antibody against botulinum LL toxin. In contrast, the mouse neutralization test detected neutralizing antibodies in sera from 1

* Corresponding author at: Human Vaccine Production Department, The Chemo-Sero-Therapeutic Research Institute (KAKETSUKEN), 1-6-1 Okubo, Kumamoto-shi, Kumamoto 860-8568, Japan. Tel.: +81 96 344 1211; fax: +81 96 345 1345.
E-mail address: torii-ya@kaketsuken.or.jp (Y. Torii).

0041-0101/$ – see front matter © 2009 Elsevier Ltd. All rights reserved.
doi:10.1016/j.toxicon.2009.09.004

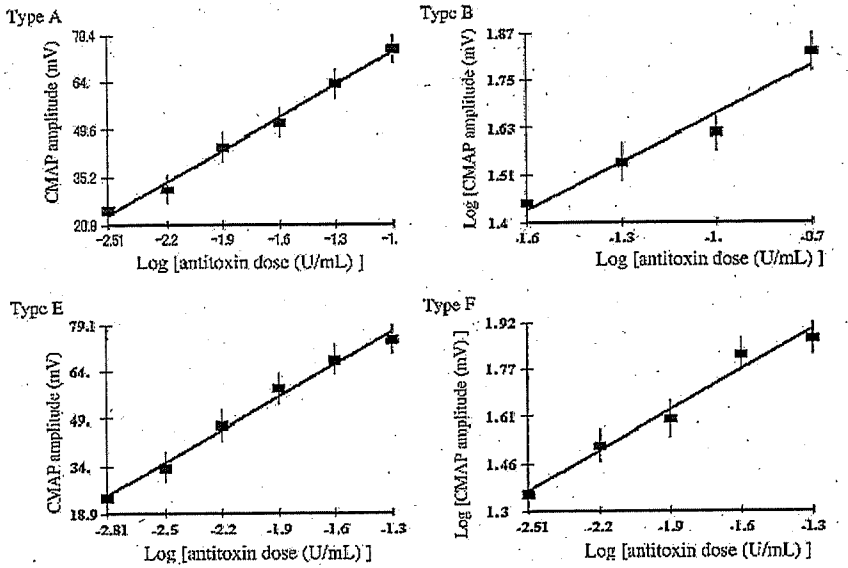

Fig. 1. Dose–response of CMAP amplitude of the test toxin mixed with standard botulinum antitoxin of each type. Rats received mixture of the antitoxin and test toxin into left gastrocnemius muscle. CMAP amplitude was measured for the left hind leg of each rat on day 1 after administration. Each point is the mean ± 95% confidence intervals, $n = 5$.

patient, showing a lower sensitivity than the CMAP neutralization test. ELISA detected neutralizing antibody presence in sera from 2 patients; however, ELISA titers were not correlated with the potency of neutralizing antibodies. This was because ELISA detected all antibodies (including non-neutralizing antibodies) against type A toxin. No antibodies were detected by these methods in the negative control. The antibody titers in serum No. 7 and the positive control detected using the CMAP and mouse neutralization tests showed similar values. Serum No. 7 was also antibody-positive on ELISA (Table 1). Comparing ELISA and the CMAP neutralization test, the correlation coefficient between the two assays was $R^2 = 0.056$ in all sera. No correlation could be identified between these titers.

Table 1
Antibody titers of sera from patients and volunteers measured using the mouse neutralization test, CMAP neutralization test, and ELISA.

Serum No.	Mouse neutralization test (mU/mL)	CMAP neutralization test (mU/mL)	ELISA[a]
1	<100	3	<2
2	<100	4	6
3	<100	4	<2
4	<100	4	<2
5	<100	4	<2
6	<100	5	<2
7	ca)100	50	3
8 (Positive control)	200	190	13
9 (Negative control)	<100	<1	<2

[a] ELISA titer expressed in multiples of the measurement from the negative control value.

As mentioned above, the CMAP neutralization test can be used for the detection of neutralizing antibodies in patients who have received treatment with type A botulinum toxin. Botulinum toxin preparations for treatment are used for various diseases in many patients. Since the therapeutic dose of botulinum toxin is very low, its therapeutic effect may be lost by only minute amounts of antibodies. For patients who show antibody presence, it may be necessary to treat them with increasing toxin doses or to change toxin types. The CMAP neutralization test may be useful to assist in such a diagnosis.

The CMAP neutralization test is capable of detecting minute amounts of neutralizing antibodies, not only against type A toxin, but also against types B, E, and F. Type A and B toxins have already been approved as formulations for the treatment of various disorders, and are currently being used in clinics. However, the effects of type E and F toxins have only recently begun to be investigated in clinical studies, and, in the future, these toxins may therefore be approved as new drugs (Mezaki et al., 1995; Eleopra et al., 1998; 2004). Thus, the ability of the CMAP test to also detect small amounts of neutralizing antibodies against type E and F toxins may be potentially useful for such toxin formulations to be developed in the future. This method is clinically applicable and useful as the measurement is simple and straight forward, using electromyographs installed at clinical sites.

Acknowledgment

The present investigation was conducted with a part of financial support from the Society for the Japan Health Sciences Foundation.

Conflicts of interest

The authors declare that there are no conflicts of interest.

References

Borodic, G., Johnson, E., Goodnough, M., Schantz, E., 1996. Botulinum toxin therapy, immunologic resistance, and problems with available materials. Neurology 46 (1), 26–29.
Byrne, M.P., Smith, T.J., Montgomery, V.A., Smith, L.A., 1998. Purification, potency, and efficacy of the botulinum neurotoxin type A binding domain from *Pichia pastoris* as a recombinant vaccine candidate. Infect. Immun. 66 (10), 4817–4822.
Casale, R., Tugnoli, V., 2008. Botulinum toxin for pain. Drugs R. D. 9 (1), 11–27.
Dressler, D., 2004. Clinical presentation and management of antibody-induced failure of botulinum toxin therapy. Mov. Disord. 19 (Suppl. 8), S92–S100.
Eleopra, R., Tugnoli, V., Rossetto, O., De Grandis, D., Montecucco, C., 1998. Different time course of recovery after poisoning with botulinum neurotoxin serotypes A and E in human. Neurosci. Lett. 256 (3), 135–138.
Eleopra, R., Tugnoli, V., Quatrale, R., Rossetto, O., Montecucco, C., 2004. Different types of botulinum toxin in humans. Mov. Disord. 19 (Suppl. 8), S53–S59.
Hatheway, C.H., Snyder, J.D., Seals, J.E., Edell, T.A., Lewis Jr., G.E., 1984. Antitoxin levels in botulism patients treated with trivalent equine botulism antitoxin to toxin types A, B, and E. J. Infect. Dis. 150 (3), 407–412.
Jankovic, J., 2004. Botulinum toxin in clinical practice. J. Neurol. Neurosurg. Psychiatr. 75 (7), 951–957.
Jones, R.G.A., Corbel, M.J., Sesardic, D., 2006. A review of WHO international standards for botulinum antitoxins. Biologicals 34 (3), 223–226.
Kessler, K.R., Benecke, R., 1997. The EDB test – a clinical test for the detection of antibodies to botulinum toxin type A. Mov. Disord. 12 (1), 95–99.
Mezaki, T., Kaji, R., Kohara, N., Fujii, H., Katayama, M., Shimizu, T., Kimura, J., Brin, M.F., 1995. Comparison of therapeutic efficacies of type A and F botulinum toxins for blepharospasm: a double-blind, controlled study. Neurology 45 (3 Pt 1), 506–508.
Sakaguchi, G., Ohishi, I., Kozaki, S., 1981. Purification and oral toxicities of *Clostridium botulinum* progenitor toxins. In: Lewis, G.E. (Ed.), Biomedical Aspects of Botulism. Academic Press, New York, pp. 21–34.
Sesardic, D., Jones, R.G., Leung, T., Alsop, T., Tierney, R., 2004. Detection of antibodies against botulinum toxins. Mov. Disord. 19 (Suppl. 8), S85–S91.
Torii, Y., Tokumaru, Y., Kawaguchi, S., Izumi, N., Maruyama, S., Mukamoto, M., Kozaki, S., Takahashi, M., 2002. Production and immunogenic efficacy of botulinum tetravalent (A, B, E, F) toxoid. Vaccine 20 (19–20), 2556–2561.
Torii, Y., Goto, Y., Takahashi, M., Ishida, S., Harakawa, T., Sakamoto, T., Kaji, R., Kozaki, S., Ginnaga, A. Quantitative determination of biological activity of botulinum toxins utilizing compound muscle action potentials (CMAP), and comparison of neuromuscular transmission blockage and muscle flaccidity among toxins. Toxicon, in press.
Truong, D.D., Jost, W.H., 2006. Botulinum toxin: clinical use. Parkinsonism Relat. Disord. 12 (6), 331–355.

J Neural Transm (2009) 116:1571–1578
DOI 10.1007/s00702-009-0304-z

BASIC NEUROSCIENCES, GENETICS AND IMMUNOLOGY - ORIGINAL ARTICLE

Accumulation of phosphorylated tyrosine hydroxylase into insoluble protein aggregates by inhibition of an ubiquitin–proteasome system in PC12D cells

Ichiro Kawahata · Hirofumi Tokuoka · Hasan Parvez · Hiroshi Ichinose

Received: 29 June 2009 / Accepted: 22 August 2009 / Published online: 12 September 2009

Abstract Tyrosine hydroxylase (TH) is a rate-limiting enzyme for the biosynthesis of catecholamines including dopamine. The relationship between proteasomal dysfunction and the etiology of Parkinson's disease has been suggested, but it is unknown if TH protein is affected by proteasomal dysfunctions. Here, we examined the effect of inhibition of ubiquitin–proteasomal pathway on biochemical characteristics of TH protein in the neuronal cells. Inhibition of 20S or 26S proteasome by proteasome inhibitor I, or MG-132 in NGF-differentiated PC12D cells induced dot-like immunoreactivities with the anti-^{40}Ser-phosphorylated TH (p40-TH) antibody. These dots were tightly co-localized with ubiquitin and positive to Thioflavine-S staining. These dot-like immunoreactivities were not obvious when immunostaining was performed against total-TH or choline acetyltransferase. Western blotting analysis showed time-dependent increase of p40-TH in the Triton-insoluble fractions. We also examined the effect of okadaic acid, an inhibitor of protein phosphatase 2A, which is a phosphatase acting on p40-TH. Okadaic acid increased the amount of insoluble p40-TH. These data suggest that p40-TH is prone to be insolubilized and aggregated by dysfunction of an ubiquitin–proteasome system in PC12D cells.

Keywords Tyrosine hydroxylase · Ubiquitin–proteasome system · MG-132 · Okadaic acid · Parkinson's disease

Abbreviations

ChAT	Choline acetyltransferase
DA	Dopamine
NGF	Nerve growth factor
OA	Okadaic acid
PD	Parkinson's disease
PKA	Cyclic AMP-dependent protein kinase (protein kinase A)
PP2A	Protein phosphatase 2A
TH	Tyrosine hydroxylase
p40-TH	Tyrosine hydroxylase phosphorylated at ^{40}Ser

Introduction

Tyrosine hydroxylase (tyrosine 3-monooxygenase, TH; EC 1.14.16.2), is a rate-limiting enzyme for biosynthesis of catecholamines (Nagatsu et al. 1964). The TH activity is strictly regulated by many factors to control the amount of dopamine. Activation by phosphorylation of the TH protein and inactivation by the binding of its end product dopamine to its active site are the two major mechanisms for regulation of the TH activity (Fujisawa and Okuno 2005). On depolarization, cyclic AMP-dependent protein kinase (PKA) and calcium-calmodulin dependent protein kinase II (CaMKII) are activated, then PKA phosphorylates TH at ^{40}Ser and

Electronic supplementary material The online version of this article (doi:10.1007/s00702-009-0304-z) contains supplementary material, which is available to authorized users.

I. Kawahata · H. Tokuoka · H. Ichinose (✉)
Graduate School of Bioscience and Biotechnology,
Tokyo Institute of Technology, 4259-B7, Nagatsuta-cho,
Midori-ku, Yokohama 226-8501, Japan
e-mail: hichinos@bio.titech.ac.jp

H. Parvez
CNRS, Institut Alfred Fessard de Neurosciences,
French National Research Centre, Gif sur Yvette, France

CAMKII phosphorylates TH at ^{19}Ser (Haycock 1990; Haycock and Haycock 1991). Phosphorylation at ^{40}Ser leads TH to liberate dopamine from its active site and change the conformation to the high-specific activity form (Daubner et al. 1992). Cytosolic free dopamine can bind to the active site of TH, and make TH inactive to suppress overproduction of dopamine (Okuno and Fujisawa 1985). It was reported that the phosphorylated form of TH was highly labile, whereas the dopamine-bound form was stable (Royo et al. 2005). Phosphorylated TH at ^{40}Ser (p40-TH) can be dephosphorylated by protein phosphatases such as protein phosphatase 2A (PP2A) (Haavik et al. 1989; Leal et al. 2002). Previously, we demonstrated that the bacterially expressed and purified TH protein, which is free from dopamine and reported to be in a similar conformation with p40-TH (Le Bourdellès et al. 1991), forms insoluble aggregates in the presence of BH4 (Urano et al. 2006).

Recent studies suggest proteasomal dysfunction and accumulation of unnecessary proteins may be one of the causes of neurodegenerative disorders such as Parkinson's disease (PD) (McNaught et al. 2001; McNaught and Olanow 2003). However, it is yet to be known if TH protein, a key enzyme of DA synthesis, is affected by proteasomal dysfunction.

In the present study, we investigated the effect of proteasomal inhibition on the TH protein using PC12D cells. We especially focused on p40-TH, because the phosphorylation on this site is more directly associated with the catalytic activity than other phosphorylation sites, Ser8, Ser19 and Ser31 (Dunkley et al. 2004). We found that proteasomal inhibition leads to accumulation of insoluble p40-TH and formation of p40-TH-containing intracellular aggregates which tightly co-localized with ubiquitin. Furthermore, inhibition of PP2A increased the amount of the p40-TH in insoluble fractions.

Materials and methods

Cell culture

PC12D cells (Katoh-Semba et al. 1987) were cultured in Dulbecco's modified Eagle's medium (DMEM; Sigma, MO, USA) containing 5% heat-inactivated fetal bovine serum (Biowest, Nuaillé, France) and 10% horse serum (JRH, KS, USA). Cells were cultured on plastic culture dishes (Falcon, NJ, USA) and incubated at 37°C with 5% CO_2. For the differentiation of PC12D cells, cells were cultured with 50 ng/ml nerve growth factor (NGF; Wako, Osaka, Japan) in the culture medium for 7 days. A 26S proteasome inhibitor, MG-132 (Calbiochem, Darmstadt, Germany), a 20S proteasome inhibitor, PSI (Calbiochem, San Diego, USA) and PP2A inhibitor, Okadaic acid (Wako, Osaka, Japan), were prepared as 250 μM or 10 mM stock solutions in dimethyl sulfoxide (DMSO). As a control, we added the same volume of DMSO.

Immunocytochemistry of cell culture

NGF-differentiated PC12D cells were incubated in culture media containing 250 nM MG-132, 10 μM PSI or DMSO for 12, 24, and 48 h. Cells were cultured on Poly-D-lysine coated culture slides (BD Biosciences, CA, USA). For double-labeled immunofluorescence analysis, PC12D cells were washed with PBS and fixed in 4% paraformaldehyde for 15 min at room temperature (RT). After washing with PBS, cells were permeabilized with 0.1% Triton X-100 in PBS for 25 min and washed with PBS. After pre-blocking in 1% BSA/PBS for 90 min, cells were incubated overnight at 4°C with the following primary antibodies; anti-TH polyclonal antibody (1:500 dilution, Millipore AB152, MA, USA), anti-^{40}Ser phosphorylated TH antibody (1:500 dilution, Cell Signaling Technology #2791S, MA, USA), anti-ubiquitin monoclonal antibody (1:100 dilution, Santa Cruz Biotechnology sc-8017, CA, USA), or anti-choline acetyltransferase (ChAT) polyclonal antibody (1:1,000 dilution, Millipore AB143). After washing with PBS, cells were incubated with Alexa Fluor 488- or 546-conjugated secondary antibodies (1:2,000 dilution, Invitrogen, CA, USA). Images were acquired by fluorescent microscopy or confocal laser microscopy (BioRad, Göttingen, Germany) using a 100× oil-immersion objective. All experiments were repeated at least three times.

Quantitative analysis of fluorescence intensity was performed using NIH ImageJ 1.39 software. First, the background signal intensities were measured from regions without any cells and subtracted from all the images. The remaining signals of cells were used to define total cell areas. We defined the inclusions as dot-like signals 3SD above the background levels and measured the areas.

Thioflavine-S staining

For Thioflavine-S staining, cells were fixed and subjected to indirect immunofluorescence staining as described above. Before mounting, cells were treated with 0.005% Thioflavine-S in 70% ethanol for 5 min. Thereafter, chambers were washed three times in 70% ethanol, once in water, and then mounted.

Western blot analyses

Naïve or NGF-differentiated PC12D cells were exposed to MG-132 (250 nM), OA (concentrations indicated in each experiment), or DMSO (control) for 2–48 h. Cells were collected using a cell scraper, washed with PBS, and

resuspended in lysis buffer consisting of 25 mM HEPES (pH 7.4), 5 mM $MgCl_2$, 1 mM EDTA, 1 mM EGTA, and 0.5% Triton X-100 with 1 μg/ml each of pepstatin and leupeptin, 0.5 mM phenylmethylsulfonyl fluoride (PMSF), and 25 mM sodium fluoride. After incubation on ice for 20 min, the insoluble material was pelleted by centrifugation at 100,000×*g* for 20 min at 4°C, resuspended in SDS-sample buffer, and boiled for 10 min. Protein concentration of both detergent-soluble and -insoluble fractions was determined by the Bradford method (BioRad, CA, USA). Twenty micrograms of protein from both fractions was separated by SDS–PAGE (10%) and transferred to a PVDF membrane, blocked in 5% non-fat milk for 1 h, and incubated overnight at 4°C with the following primary antibodies; anti-TH polyclonal antibody (1:1,000 dilution, Millipore AB152), anti-^{40}Ser phosphorylated TH antibody (1:1,000 dilution, Cell Signaling Technology #2791S), anti-ubiquitin monoclonal antibody (1:200 dilution, Santa Cruz Biotechnology sc-8017), or anti-β-actin monoclonal antibody (1:10,000 dilution, Sigma A5441). Immunoreactive bands were visualized with horseradish peroxidase-conjugated secondary antibodies (1:30,000 dilution, GE Healthcare Life Sciences, Uppsala, Sweden) and the chemiluminescent HRP substrate (Millipore, Massachusetts, USA). Visualized bands were detected by LAS-3000 mini (Fujifilm, Tokyo, Japan).

Quantitative analysis by densitometry was performed using Multi Gauge Ver.2.11 software (Fujifilm). Intensity of the bands between MG-132 treated and vehicle treated PC12D cells were compared after subtracting background signals (arbitrary unit per square mm, a.u./mm^2). All experiments were repeated four times. Statistical significance was calculated according to Student's *t* test.

Results

Proteasomal inhibition leads to formation of p40-TH positive insoluble aggregates

We first investigated the effects of proteasomal inhibition on the TH protein by immunocytochemistry in NGF-differentiated PC12D cells. Cells were cultured for 7 days with NGF, then exposed to a 26S proteasome inhibitor, MG-132, at 250 nM for up to 48 h. Under the condition, cells showed no drastic morphological alterations (data not shown). We stained the cells with an antibody against p40-TH to examine a possible alteration in the cellular localization of p40-TH. We found that the p40-TH antibody showed dot-like immunoreactivities from 12 h after MG-132 treatment, suggesting the generation of protein aggregates containing p40-TH (Fig. 1a, p40-TH). In double-staining with the p40-TH antibody and the antibody against ubiquitin, most of p40-TH positive signals were tightly co-localized with the ubiquitin signals (Fig. 1a, p40-TH/Ubi). The p40-TH immunopositive spots increased their size in a time-dependent manner (Fig. 1b, top). Images with lower magnification were shown in supplementary figure (Suppl Fig. 1). We also examined the effect of proteasomal inhibition with another reagent PSI, an inhibitor of 20S proteasome, and the similar trends were observed under the same condition as MG-132 experiments (Suppl Fig. 2).

When we examined the immunoreactivity with the polyclonal antibody against total-TH protein, the signal accumulated more slowly than that of p40-TH, and finally formed larger signals than the p40-TH immunoreactivities (Fig. 1a, TH/Ubi). Total-TH positive areas were larger than those of ubiquitin, whereas most of ubiquitin positive ones were TH immunoreactive (Fig. 1a, TH/Ubi). Areas of p40-TH immunoreactivities were smaller in size, but their signals were stronger and denser than those of TH by fluorescence quantification (data not shown).

In contrast, immunoreactivities against ChAT showed no dot-like signals as seen in the p40-TH (Fig. 1a, ChAT/Ubi). Furthermore, ChAT did not co-localize with any ubiquitin marker (Fig. 1a, ChAT/Ubi). We also performed the experiments in the NGF-untreated cells and the similar results were obtained (data not shown).

To further characterize the p40-TH immunopositve signals, we counter-stained the MG-132 treated cells with Thioflavine-S, an insoluble aggregate marker. Most p40-TH immunoreactivities were co-localized with Thioflavine-S (Fig. 2), suggesting the p40-TH positive dot-like signals were protein aggregates.

Taken together, these data suggest that p40-TH is more preferentially incorporated to Thioflavine-S- and ubiquitin-positive aggregates by proteasome inhibition, than non-phosphorylated-TH and ChAT.

Proteasomal inhibition leads to time-dependent increase in the amount of insolubilized p40-TH

We then examined if the p40-TH-containing aggregates, which was detected by immunocytochemistry, is detergent-soluble or not by Western blotting. After treatment with MG-132, cells were homogenized in presence of 0.5% Triton X-100, separated to soluble and insoluble fractions by ultra-centrifugation at 100,000 × *g*, and subjected to Western blot analyses. The intensity of p40-TH immunoreactive band in the Triton-X soluble component was slightly increased in MG-132 treated cells. In contrast, the p40-TH positive signal in the insoluble fraction was detected 12 h after MG-132 treatment, and increased dramatically in a time-dependent manner, though almost no signal was detected in the control insoluble fractions (Fig. 3a, p40-TH). Inhibition of proteasomal activity by MG-132 was confirmed by the accumulation of ubiquitin-positive signals in

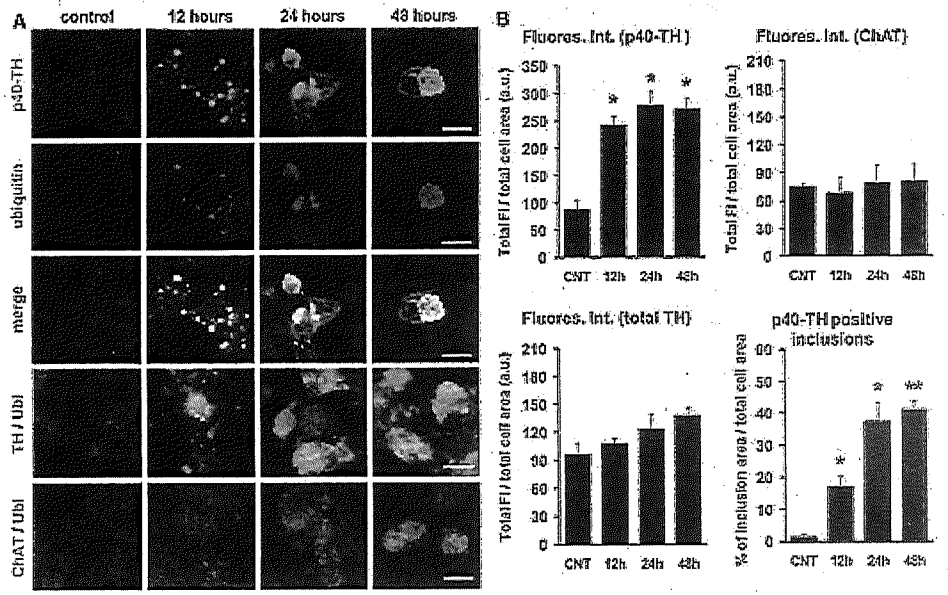

Fig. 1 26S proteasomal inhibition induces formation of p40-TH positive cytoplasmic aggregates. **a** Representative immunofluorescence staining of MG-132-treated PC12D cells. MG-132 treatment induced aggregation of p40-TH and formation of its positive inclusions. Immunoreactive spots of p40-TH tightly co-localized with those of ubiquitin. Ubiquitin immunoreactive signals were smaller than TH positive ones and most of them were included in the TH immunoreactive area. The antibody against ChAT did not show the formation of aggregates and no specific co-localization with any ubiquitin marker. Scale bars, 10 μm. **b** Quantification of fluorescence intensities shown in **a**. Fluorescence intensities per cell area for p40-TH, total-TH, and ChAT, and the ratios of strong p40-TH positive areas (beyond 3 SD of control signal) per total cell area were shown. The areas of p40-TH positive inclusions were increased time-dependently, but ChAT positive ones were not. Measurement for the area was carried out with NIH ImageJ software. *CNT* control, *V* vehicle treatment (DMSO). Values represent mean ± SD; $n = 3$. $^*p < 0.05$, $^{**}p < 0.01$ compared to control. All cells were differentiated with 50 ng/mL NGF for 7 days and exposed to 250 nM MG-132 for indicated hours

the insoluble fractions (Fig. 3a, ubiquitin). The alteration in the amount of total-TH protein was not drastic (Fig. 3a, TH). No significant change was observed in the β-actin levels (Fig. 3a, β-actin). Quantitative analysis revealed that insoluble component of p40-TH was increased to about 15-fold of the control 48 h after the addition of MG-132, but total-TH showed no significant difference (Fig. 3b). We also calculated the ratios for the Triton-insoluble to Triton-soluble components of p40-TH and total-TH in Fig. 3c. These data indicate that p40-TH is prone to be insolubilized compared with non-phosphorylated TH under the condition of proteasomal dysfunction.

PP2A inhibition also leads to accumulation of insoluble p40-TH

In order to clarify whether the occurrence of insoluble p40-TH aggregates was caused by the characteristics of p40-TH itself or by the effects of other proteins which were accumulated due to the inhibition of proteasome, we treated PC12D cells with okadaic acid (OA), an inhibitor of PP2A, which reportedly dephosphorylates p40-TH (Haavik et al. 1989; Leal et al. 2002). First, PC12D cells were exposed to different concentrations of OA for 24 h, and then homogenates were separated to Triton-insoluble and -soluble components by ultra-centrifugation and analyzed by Western blotting. By increasing the concentration of OA from 10 to 250 nM, the amount of p40-TH in Triton-insoluble components increased in a dose-dependent manner (Fig. 4a, c, p40-TH). Next, cells were treated with 250 nM OA for various hours. Insoluble p40-TH was detected 6 h after the addition of OA, and the amount of insoluble p40-TH increased time-dependently (Fig. 4b, d, p40-TH). The amount of total-TH protein showed no significant alteration in both the Triton-soluble and -insoluble fractions (Fig. 4a–d, TH). The proportion of insoluble component to soluble component was

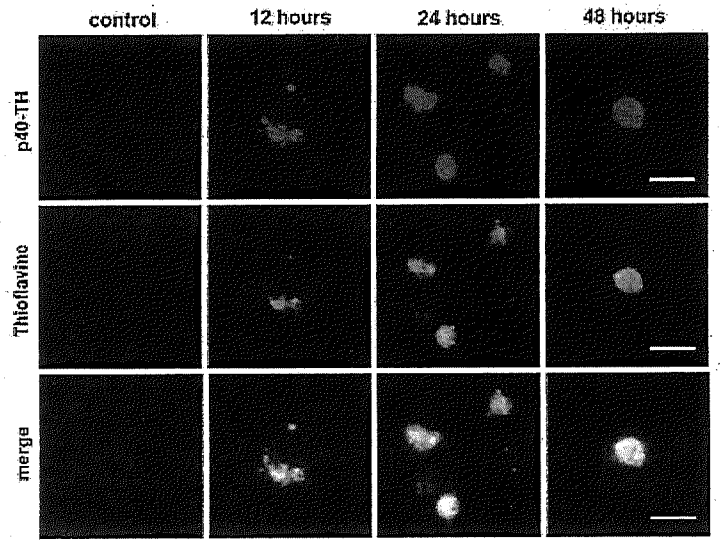

Fig. 2 Localization of p40-TH immunoreactivity and Thioflavine-S positive aggregates in NGF-differentiated PC12D cells. PC12D cells were grown with NGF to differentiate for 1 week then exposed to 250 nM MG-132 for indicated hours. Thioflavine-S positive aggregates appeared in 12 h, and they are smaller than p40-TH immunoreactive spots and partially co-localized. Tight co-localization of p40-TH immunoreactivity and Thioflavine-S positive aggregates was observed from 24 h. *Scale bars* 10 μm

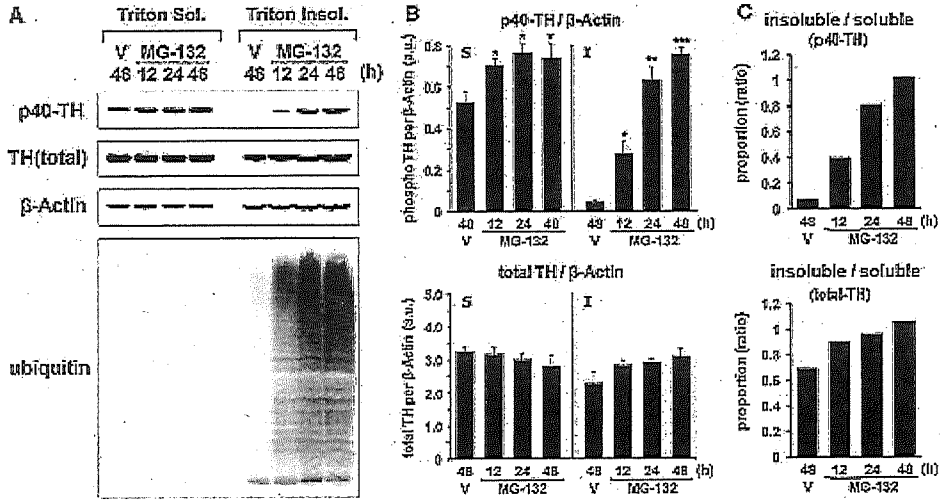

Fig. 3 Western blot analysis of the effect of 26S Proteasomal inhibition on p40-TH solubilization. a NGF-differentiated PC12D cells were treated with MG-132 for indicated hours, fractionated to Triton X-100-soluble and -insoluble fractions, and subjected to Western blotting. b Summary of quantification for the immunoreactivities on panel a. Without MG-132, most p40TH was in soluble fractions, while treatment with MG-132 lead to accumulation of p40-TH in insoluble fractions in a time-dependent manner. No significant alteration was observed with total-TH and β-actin though modest increase of insoluble component was observed in total-TH. Values represent mean ± SD; $n = 3$ in all experiments. $^{*}p < 0.05$, $^{**}p < 0.01$, $^{***}p < 0.005$ compared to control "V". *V* vehicle treatment, *S* Triton X-100-soluble fraction, and *I* triton-insoluble fraction, respectively. c The proportion for the triton-soluble and -insoluble component in p40-TH and total-TH under the basal conditions and in the presence of the MG-132, a 26S proteasomal inhibitor

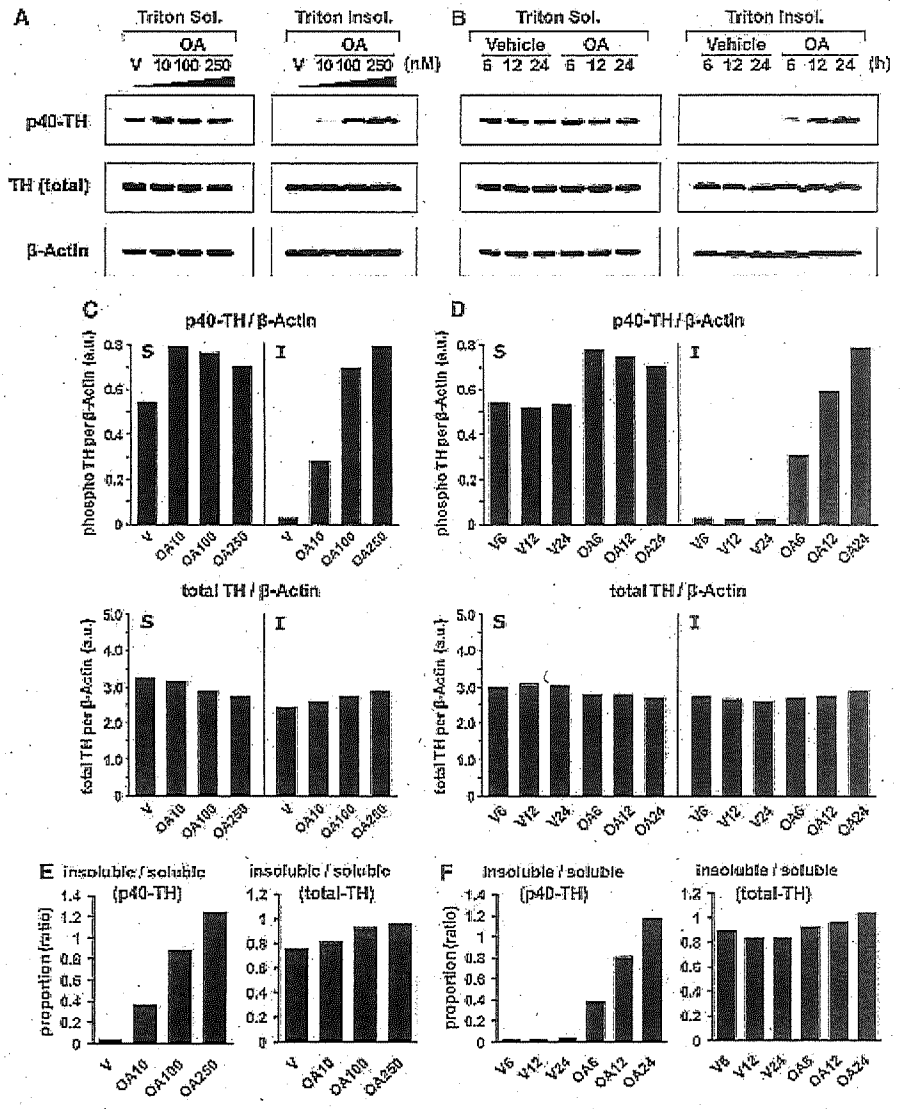

Fig. 4 Increase in insoluble component of p40-TH by PP2A inhibition with OA. a PC12D cells were treated with indicated concentrations of OA for 24 h, and subjected to Western blotting analysis. PP2A inhibition induced a dose-dependent accumulation of insoluble p40-TH, as observed in MG-132 treatment. b PC12D cells were treated with 250 nM OA for indicated hours, and subjected to Western blotting analysis. Insoluble p40-TH was accumulated time-dependently. No apparent alteration was observed in total-TH level. Vehicle, *OA* okadaic acid. (c, d) Summary of quantification for the immunoreactivities shown in a and b. (e, f) The proportion for the triton-soluble and -insoluble component in p40-TH and total-TH under the basal conditions and in the presence of okadaic acid, an inhibitor of PP2A

compared between p40-TH and total-TH, and it indicates that the increase rate of insolubilization was more drastic in p40-TH (Fig. 4e, f). These results suggest that p40-TH protein tends to be easily insolubilized and accumulate in the cell.

Discussion

In this study, we investigated the effect of proteasomal dysfunction on the TH protein in PC12D cells. We demonstrated for the first time that p40-TH was insolubilized and aggregated in living neuronal cells by proteasomal inhibition and PP2A inhibition. These aggregates were positive for Thioflavine-S and co-localized with ubiquitin. Our present data show that p40-TH is prone to make insoluble aggregates in the cells, although it is not clear whether the aggregates are constituted of p40-TH alone or with many other proteins.

Our group previously showed that recombinant TH protein expressed in *Escherichia coli* had tendency to be easily aggregated in vitro (Urano et al. 2006). It has been reported that the bacterially expressed TH protein showed enzymatic properties that were similar to p40-TH, because both p40-TH and bacterially expressed TH are free from the bound dopamine (Le Bourdellès et al. 1991; Fujisawa and Okuno 2005). Thus, our results on insoluble aggregates of p40-TH in PC12D cells are in good accordance with our previous in vitro results, and suggest that the aggregation of the p40-TH protein may occur in living neuronal cells.

Phosphorylation sites of TH are within the first 40 amino acid residues in the flexible N-terminal domain (Dunkley et al. 2004), and deletion of the N-terminal region was reported to stabilize the TH protein (Nakashima et al. 2005). These findings suggest that a conformational change induced by the phosphorylation at ^{40}Ser may make the TH protein labile and prone to be aggregated.

Increases in the amount of soluble p40-TH were not prominent in the cells treated with okadaic acid (Fig. 4). We treated the cells with okadaic acid for relatively longer period (6–24 h), because we did not detect any insoluble p40TH less than 6 h and we thought that it might take time to form triton-insoluble inclusions in the cells. Thus, it would be possible that a feed-back regulation to reduce the excess amount of p40TH happened in the cells. It would be noteworthy that slight increase in the amount of p40-TH and/or alteration in the metabolism of p40-TH resulted in the increases of insoluble p40-TH.

We showed inhibition of 20S or 26S proteasome induced the accumulation of insoluble component of p40-TH. This result raises possibility that p40-TH may be degraded by ubiquitin–proteasome system. Interestingly, mono-ubiquitination of TH protein was reported using recombinant TH protein, which is presumably DA-free like p40-TH (Døskeland and Flatmark 2002). Thus, p40-TH may be ubiquitinated under normal condition, and inhibition of proteasome may cause accumulation of excess p40-TH which in turn forms insoluble aggregates.

26S proteasome-mediated protein degradation can be impaired by α-Syn protofibrils (Zhang et al. 2008). In addition, the impairment of proteasome function is supposed to be age-dependent (Carrard et al. 2002; Keller et al. 2002). Such failure of the ubiquitin–proteasome system, which would induce an accumulation and aggregation of cytoplasmic proteins, may play a major role in the pathogenesis of both familial and sporadic forms of PD (McNaught et al. 2001; McNaught and Olanow 2003), perhaps mediated by cellular inflammation (Wersinger and Sidhu 2002). Further studies will clarify the possible relevance of the regulation of TH phosphorylation and degradation with pathogenesis of neurodegenerative disorders.

Several reports showed that Lewy bodies were immunopositive to anti-TH antibody in locus ceruleus (Nakashima and Ikuta 1984), cerebral cortex (Kuljis et al. 1989) and substantia nigra (Kawahata et al. 2009). α-Synuclein (α-Syn) is a major component of Lewy bodies, and the deposition of α-Syn is a hallmark of a subset of neurodegenerative disorders including PD (Ueda et al. 1993; Spillantini et al. 1997, 1998). Since α-Syn is expressed not only in the nigrostriatal dopaminergic neurons, but also in the cerebral cortex and other cholinergic neurons (Maroteaux et al. 1988), this alone cannot explain the selective neuronal degeneration in PD. Given that TH is expressed selectively in catecholaminergic neurons, the tendency of p40-TH protein to form insoluble aggregates may be relevant to the selective degeneration of dopaminergic neurons in PD. It would be important to investigate the interaction of α-Syn and phosphorylated TH, although we could not examine it in this study because PC12D cells express little amount of α-Syn. We recently found p40-TH positive immunoreactivities in the substantia nigra from an autopsied brain of a PD patient (Kawahata et al. 2009). In the future studies, we would explore whether presence of the p40-TH protein may make dopaminergic neurons vulnerable to damages caused by proteasomal dysfunction.

Acknowledgments This work was supported by the Research Grant (18A-2) for Nervous and Mental Disorders from the Ministry of Health, Labor and Welfare of Japan; by grants from the Ministry of Education, Culture, Sports, Science, and Technology of Japan; and by JST, CREST.

References

Carrard G, Bulteau AL, Petropoulos I, Friguet B (2002) Impairment of proteasome structure and function in aging. Int J Biochem Cell Biol 34:1461–1474

Daubner SC, Lauriano C, Haycock JW, Fitzpatrick PF (1992) Site-directed mutagenesis of serine 40 of rat tyrosine hydroxylase. J Biol Chem 267:12639–12646

Døskeland AP, Flatmark T (2002) Ubiquitination of soluble and membrane-bound tyrosine hydroxylase and degradation of the soluble form. Eur J Biochem 269:1561–1569

Dunkley PR, Bobrovskaya L, Graham ME, Nagy-Felsobuki EI, Dickson PW (2004) Tyrosine hydroxylase phosphorylation: regulation and consequences. J Neurochem 91:1025–1043

Fujisawa H, Okuno S (2005) Regulatory mechanism of tyrosine hydroxylase activity. Biochem Biophys Res Commun 338: 271–276

Haavik J, Schelling DL, Campbell DG, Andersson KK, Flatmark T, Cohen P (1989) Identification of protein phosphatase 2A as the major tyrosine hydroxylase phosphatase in adrenal medulla and corpus striatum: evidence from the effects of okadaic acid. FEBS Lett 251:36–42

Haycock JW (1990) Phosphorylation of tyrosine hydroxylase in situ at serine 8, 19, 31, and 40. J Biol Chem 265:11682–11691

Haycock JW, Haycock DA (1991) Tyrosine hydroxylase in rat brain dopaminergic nerve terminals. J Biol Chem 266:5650–5657

Katoh-Semba R, Kitajima S, Yamazaki Y, Sano M (1987) Neuritic growth from a new subline of PC12 pheochromocytoma cells: cyclic AMP mimics the action of nerve growth factor. J Neurosci Res 17:36–44

Kawahata I, Yagishita S, Hasegawa K, Natatsu I, Nagatsu T, Ichinose H (2009) Immunohistochemical analyses of human brain-stem type Lewy bodies and the localization of phosphorylated tyrosine hydroxylase in the midbrain. Biogenic Amines (in press)

Keller JN, Gee J, Ding Q (2002) The proteasome in brain aging. Ageing Res Rev 1:279–293

Kuljis RO, Martín-Vasallo P, Peress NS (1989) Lewy bodies in tyrosine hydroxylase-synthesizing neurons of the human cerebral cortex. Neurosci Lett 20:49–54

Le Bourdellès B, Horellou P, Le Caer JP, Denèfle P, Latta M, Haavik J, Guibert B, Mayaux JF, Mallet J (1991) Phosphorylation of human recombinant tyrosine hydroxylase isoforms 1 and 2: an additional phosphorylated residue in isoform 2, generated through alternative splicing. J Biol Chem 266:17124–17130

Leal RB, Sim AT, Gonçalves CA, Dunkley PR (2002) Tyrosine hydroxylase dephosphorylation by protein phosphatase 2A in bovine adrenal chromaffin cells. Neurochem Res 27:207–213

Maroteaux L, Campanelli JT, Scheller RH (1988) Synuclein: a neuron-specific protein localized to the nucleus and presynaptic nerve terminal. J Neurosci 8:2804–2815

McNaught KS, Olanow CW (2003) Proteolytic stress: a unifying concept for the etiopathogenesis of Parkinson's disease. Ann Neurol 53(Suppl. 3):73–86

McNaught KS, Olanow CW, Halliwell B, Isacson O, Jenner P (2001) Failure of the ubiquitin–proteasome system in Parkinson's disease. Nat Rev Neurosci 2:589–594

Nagatsu T, Levitt M, Udenfriend S (1964) Tyrosine hydroxylase the initial step in norepinephrine biosynthesis. J Biol Chem 239:2910–2917

Nakashima S, Ikuta F (1984) Tyrosine hydroxylase protein in Lewy bodies of parkinsonian and senile brains. J Neurol Sci 66:91–96

Nakashima A, Hayashi N, Kaneko YS, Mori K, Egusa H, Nagatsu T, Ota A (2005) Deletion of N-terminus of human tyrosine hydroxylase type 1 enhances stability of the enzyme in AtT-20 cells. J Neurosci Res 81:110–120

Okuno S, Fujisawa H (1985) A new mechanism for regulation of tyrosine 3-monooxygenase by end product and cyclic AMP dependent protein kinase. J Biol Chem 260:2633–2635

Royo M, Fitzpatrick PF, Daubner SC (2005) Mutation of regulatory serines of rat tyrosine hydroxylase to glutamate: effects on enzyme stability and activity. Arch Biochem Biophys 434:266–274

Spillantini MG, Schmidt ML, Lee VM, Trojanowski JQ, Jakes R, Goedert M (1997) α-Synuclein in Lewy bodies. Nature 388:839–840

Spillantini MG, Crowther RA, Jakes R, Hasegawa M, Goedert M (1998) α-Synuclein in filamentous inclusions of Lewy bodies from Parkinson's disease and dementia with Lewy bodies. Proc Natl Acad Sci USA 95:6469–6473

Ueda K, Fukushima H, Masliah E, Xia Y, Iwai A, Yoshimoto M, Otero DA, Kondo J, Ihara Y, Saitoh T (1993) Molecular cloning of cDNA encoding an unrecognized component of amyloid in Alzheimer disease. Proc Natl Acad Sci USA 90:11282–11286

Urano F, Hayashi N, Arisaka F, Kurita H, Murata S, Ichinose H (2006) Molecular mechanism for pterin-mediated inactivation of tyrosine hydroxylase: formation of insoluble aggregates of tyrosine hydroxylase. J Biochem 139:625–635

Wersinger C, Sidhu A (2002) Inflammation and Parkinson's disease. Curr Drug Targets Inflamm Allergy 1:221–242

Zhang NY, Tang Z, Liu CW (2008) α-Synuclein protofibrils inhibit 26 S proteasome-mediated protein degradation: understanding the cytotoxicity of protein protofibrils in neurodegenerative disease pathogenesis. J Biol Chem 283:20288–20298

Contents lists available at ScienceDirect

Parkinsonism and Related Disorders

journal homepage: www.elsevier.com/locate/parkreldis

Review

Identification and management of deep brain stimulation intra- and postoperative urgencies and emergencies☆

Takashi Morishita [a,c], Kelly D. Foote [b], Adam P. Burdick [b], Yoichi Katayama [c,d], Takamitsu Yamamoto [c,d], Steven J. Frucht [e], Michael S. Okun [a,b,*]

[a] Department of Neurology, University of Florida College of Medicine/Shands Hospital, Movement Disorders Center, McKnight Brain Institute, Gainesville, FL, USA
[b] Department of Neurosurgery, University of Florida College of Medicine/Shands Hospital, Movement Disorders Center, McKnight Brain Institute, Gainesville, FL, USA
[c] Department of Neurological Surgery, Nihon University School of Medicine, Tokyo, Japan
[d] Division of Applied System Neuroscience, Department of Advanced Medical Science, Nihon University School of Medicine, Tokyo, Japan
[e] Department of Neurology, Columbia University College of Physicians and Surgeons/Columbia-Presbyterian Medical Center, New York, NY, USA

ARTICLE INFO

Article history:
Received 30 June 2009
Received in revised form
23 September 2009
Accepted 1 October 2009

Keywords:
Deep brain stimulation
Movement disorders
Emergency
Differential diagnosis
Adverse event

ABSTRACT

Deep brain stimulation (DBS) has been increasingly utilized for the therapeutic treatment of movement disorders, and with the advent of this therapy more postoperative urgencies and emergencies have emerged. In this paper, we will review, identify, and suggest management strategies for both intra- and postoperative urgencies and emergencies. We have separated the scenarios into 1 – surgery/procedure related, 2 – hardware related, 3 – stimulation-induced difficulties, and 4 – others. We have included ten illustrative (and actual) case vignettes to augment the discussion of each issue.

Contents

☆ The review of this paper was entirely handled by the Co-Editor-in-Chief, Zbigniew Wszolek.

* Corresponding author at: Department of Neurology, McKnight Brain Institute, Medical Director National Parkinson Foundation, 100 S Newell Dr, Room L3-101, Gainesville, FL 32610, USA. Tel.: +1 352 273 5550; fax: +1 352 273 5575.
E-mail address: okun@neurology.ufl.edu (M.S. Okun).

1353-8020/$ – see front matter © 2009 Elsevier Ltd. All rights reserved.
doi:10.1016/j.parkreldis.2009.10.003

1. Introduction

Neurosurgical procedures for basal ganglia disorders may result in urgent or emergent management issues. Postoperative urgencies and/or emergencies should be identified and treated in an expeditious manner. Deep brain stimulation (DBS) has been increasingly utilized for addressing neurologic and neuropsychiatric disorders [1,2], and with the increasing number of DBS cases being performed each year, there has been a commensurate increase in the number of issues relating to the surgical, the procedural, and to the stimulation-related phenomena. Some of these issues have manifested themselves as movement disorders (e.g. dyskinesia, ballism, dystonia), although the majority have presented in other ways [3–5]. In this paper, we have separated the potential scenarios into 1 – surgery/procedure related, 2 – hardware related, and 3 – stimulation-induced phenomena. The discussion has been augmented by the use of clinical vignettes which illustrate the diagnosis and management of both urgent and emergent situations. Complications of DBS have unique manifestations, and diagnostic criteria and management have not been fully established in some cases. Therefore, it is possible that clinicians may overlook DBS-induced complications, and delay the appropriate management. This delay may unnecessarily result in secondary complications. The aim of this paper is to review urgent and emergent DBS-associated situations to provide recommendations for appropriate management.

2. Methods

Complications with DBS-specific manifestations have been specifically selected for this review, and a PubMed based literature search was performed for each issue. We queried the Institutional Review Board (IRB) approved DBS database of University of Florida Movement Disorders Center (UFMDC) for the illustrative cases from the period between July 2002 and June 2009.

2.1. Surgery/procedure related urgencies/emergencies

2.1.1. Intracranial hemorrhage

Case 1. A 73-year-old man with a 16-year-history of Parkinson's disease (PD) underwent unilateral subthalamic nucleus (STN) lead implantation. There was no history of hypertension, diabetes mellitus (DM), or coronary artery disease (CAD). Following the procedure, he became somnolent, and a postoperative computed tomography (CT) scan revealed a hematoma in the left lateral ventricle (Fig. 1B). There was involvement of the third ventricle and the Sylvian aqueduct. The patient developed acute obstructive hydrocephalus that necessitated emergent ventriculostomy. He convalesced for one week postoperatively, and then developed a deep venous thrombosis, an aspiration pneumonia, atrial fibrillation, a urinary tract infection, and sepsis. The total hospitalization was extended to 40 postoperative days. Following eight months of rehabilitation and anticoagurant therapy he has recovered, and implantation of Implantable Pulse Generator (IPG) was scheduled.

Hemorrhage is an emergent adverse event that may be seen following DBS, and may result in significant morbidity or rarely even death. Hemorrhages following DBS may include intracerebral (ICH), intraventricular (IVH), subdural (SDH), subarachnoid (SAH) and epidural (EDH) (Fig. 1). Hemorrhagic complications have been assumed to be due to damage to the blood vessels by the microelectrode recordings (MERs) and/or macrostimulation passes, and it has been discussed that multiple MERs and/or macrostimulation passes may increase the incidence of hemorrhagic complications (debated but generally accepted among the experts) [6–8]. Intracranial hemorrhage can be diagnosed by CT scan which may be sought in the postoperative period and is usually performed as a result of a mental status change and/or a focal neurological deficit. The incidence of hemorrhage varies from 0.6 to 3.3% [7,9–13]. Intracranial hemorrhage can precipitate secondary complications such as pneumonia, pulmonary embolus, and urinary tract infection. A recent German multicenter study revealed an overall 30-day postoperative mortality rate of 0.4% (5 of 1183 patients), and mortality due to hemorrhage in 2 of 5 patients [14]. Delay of identification and management of ICH can result in significant morbidity, therefore emergent care should be employed to prevent both primary and secondary complications. When ICH is encountered it mandates immediate neurosurgical consultation, preferably by the neurosurgeon who implanted the DBS system, although this is not always possible. Most patients can be managed conservatively, however if operative intervention for evacuation is deemed necessary every attempt should be made not to remove the DBS hardware (Table 1). Patients requiring evacuation as well as those not requiring surgery have the potential for good recovery.

2.1.2. Venous infarction

Case 2. A 60-year-old man with PD underwent a staged unilateral globus pallidus interna (GPi) DBS. He was discharged on postoperative day #1 following an uncomplicated hospital course, but later that day he began to develop left-sided weakness, lethargy, and confusion which peaked on postoperative day #2. He presented to the emergency room (ER) on postoperative day #4. A head CT scan revealed hemorrhage spreading from the center of the DBS lead. The region was surrounded by edema (Fig. 1D). The diagnosis of venous infarction was made and he was conservatively managed. Following several months, his neurological status returned to baseline, and his DBS was effectively programmed to address both motor fluctuations and parkinsonism.

Venous infarction has been associated with damage to a cortical vein that may occur during DBS surgery. Cerebral edema and hemorrhage may slowly develop and are usually the result of venous stasis or venous hypertension. These phenomena are thought to occur as a result of venous obstruction which usually traces to the damaged cortical vein. Venous infarction can be characterized by a delayed clinical onset with edema and possibly hemorrhage along the path of the DBS lead [15]. These features may be absent in some cases. Importantly, the head CT may not reveal an obvious lesion in the immediate postoperative period, and a repeat CT may be necessary to confirm diagnosis. The prognosis is usually positive in venous infarction occurring post-DBS [7,16]. Careful preoperative targeting using a high quality contrasted MRI will aid in avoiding cortical veins, and may prevent this complication [7]. If the diagnosis of venous infarction is made postoperatively, the management should include optimizing the venous return (e.g. elevate the head of the bed), managing blood pressure, avoiding dehydration, and initiating early rehabilitation (Table 1).

2.1.3. Dyskinetic storm

Postoperative dyskinesia is a relatively common phenomenon associated with STN DBS, especially in PD patients who preoperatively suffered from severe medication-induced dyskinesia [4]. Microelectrode recording, cannula placement and/or lead placement may all induce dyskinesias especially in patients with PD. Acute and severe exacerbation of dyskinesias (dyskinetic storm) in the operative setting has been previously reported and may be a feature associated with a positive prognosis [3]. In severe cases, dyskinesia may be associated with dyspnea and rhabdomyolysis [17,18], and emergent administration of sedative agents (such as IV propofol) may be required [3] (Table 1). Dyskinesia may also be induced by DBS placement in a delayed fashion [19], and dyskinetic storm may be encountered in the clinical setting following DBS programming. Management of dyskinesia in the clinical settings will also be discussed in the "*Stimulation-related motor symptoms*" section of this review.

2.1.4. Postoperative behavioral and cognitive problems

Postoperative cognitive and behavioral decline is a common DBS-related adverse event. It is usually temporary, but in patients with preoperative cognitive dysfunction it may persist. The incidence of confusion has been recently reported as 5% in a large single center study [20], but rates may vary depending on preoperative comorbidities, target site, and whether staging of operative sides is employed (i.e., as opposed to same-day simultaneous bilateral DBS implantation) [4,21–23]. The incidence of behavioral and cognitive problems may be higher in STN DBS when compared to other targets [4,23–25]. A recent randomized double-blind study revealed a higher incidence of cognitive adverse events in patients with STN DBS when compared to GPi DBS [23]. Also verbal fluency seemed worse in STN and the change was reported as more surgery-related rather than a stimulation-related effect (i.e. it occurred in the off STN condition as well as the on STN DBS condition during blinded testing) [23].

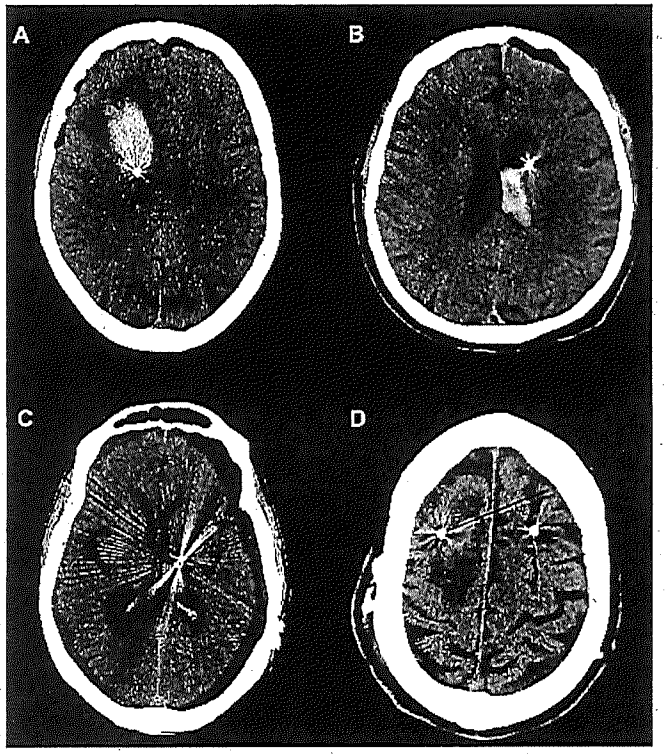

Fig. 1. Computed tomography (CT) scan images of the many types of hemorrhage that may be encountered following DBS lead implantation. This panel of CT images reveals examples of intracerebral hemorrhage (A), intraventricular hemorrhage (B), subdural hemorrhage (C), and venous infarction (D).

Anticholinergics (including not only anti-Parkinsonian medications but also medications for neurogenic bladder) may also increase the risk of postoperative cognitive problems, and may need to be discontinued [26]. It is important for clinicians to keep in mind that advanced age and/or pre-existing neurological compromise may predispose patients to mental status changes following DBS, and this is a compelling reason for centers to perform preoperative neuropsychological screening [21].

The management of postoperative behavioral and cognitive problems should include a diagnostic workup of potential underlying causes that may exacerbate and/or contribute to the clinical condition. These may include urinary tract infections, hemorrhage or medications related phenomena. If no underlying treatable cause can be identified, the clinician should utilize pharmacotherapy and a multi/interdisciplinary approach to manage the behavioral change(s). This approach may be facilitated in select cases by an inpatient admission.

Patients may become restless and violent postoperatively due to hallucinations/delusions, and this situation may require urgent/emergent care. In these cases, conventional neuroleptics are usually contraindicated, however using selective dopaminergic blockers such as quetiapine or clozapine may be useful [27] (Table 1). Non-selective dopaminergic blockers (e.g. olanzapine, risperidone, haloperidol, etc.) that have been commonly employed for the treatment of behavioral emergencies have also been observed to lead to drug-induced parkinsonism as well as other movement disorders [28,29].

2.1.5. Suicide attempt or ideation

Case 3. A 54-year-old woman with PD and depression who had a left DBS implantation two years prior to presentation was brought to the emergency room following a suicide attempt by drug overdose. Passive suicidal ideation was noted on her psychiatric evaluation prior to DBS.

Several reports have revealed cases of attempted and completed suicide occurring following DBS [30–32]. DBS may increase the risk of suicide when compared to the general population, but not necessarily when compared to a PD population (without DBS) [31,33]. A recent multicenter study revealed that preoperative history of impulse control disorders or compulsive medication use, postoperative depression, postoperative apathy, and being single were strongly associated with suicide attempts [33]. Previous suicide attempts, younger age of the patient, and younger onset of PD were also revealed to be associated with suicide attempt within the same study cohort. Therefore, screening for suicidal ideation following DBS should be routine, and if discovered, it should be treated as an emergency. Clinicians should admit patients to the hospital for multi/interdisciplinary care, which may include cognitive behavioral therapy, counseling, and/or medication/stimulation adjustment(s) (Table 1). Whether DBS results in disinhibition or impulsiveness and ultimately contributes to suicidal ideation or suicide remains controversial [34]. Vigilant pre and postoperative screening for depression and suicidal ideation are recommended. Preoperative neuropsychological and psychiatric evaluation is highly recommended as a preventative measure [21,32]. Advanced PD patients are likely to have cognitive and/or mood disturbances, and neuropsychologists can play an important role for screening out these issues. Recently, there have been several reports of suicide in dystonia DBS highlighting that this issue may not be solely related to PD [30,31,35].

2.1.6. Myocardial infarction

Case 4. A 58-year-old male with PD, coronary artery disease (CAD) (previously treated with angioplasty), hypertension, diabetes mellitus (DM), and hyperlipidemia underwent unilateral STN DBS placement. An implantable pulse generator (IPG) was placed four weeks following the DBS lead. Following IPG implantation

Table 1
Postoperative surgery and hardware related urgencies and emergencies.

Issue	Routine/urgent/emergent	Management
Intracerebral hemorrhage	Emergent	If the hemorrhage is very large, an emergent craniotomy may need to be performed.
Intraventricular hemorrhage	Emergent	Ventriculostomy if necessary may be performed for obstructive hydrocephalus.
Subdural hematoma	Emergent	If acute and symptomatic, an emergent craniotomy may be performed in select cases. If chronic, a burr hole irrigation may be performed, or it may be watched conservatively.
Epidural hematoma	Emergent	An emergent craniotomy should be performed immediately in severe cases.
Venous infarction	Urgent/emergent	Conservative therapy. An emergent craniotomy may be performed if hemorrhage is life threatening.
Dyskinetic storm	Urgent	Sedative agents may be administered in select cases. Reducing the dopaminergic medication may help. In some cases ICU care is necessary.
Behavioral/cognitive issues	Urgent/emergent	Identify and treat the underlying issues. Selective dopamine blockers (e.g. quetiapine, clozapine) may be used, but non-selective blockers should be avoided if possible.
Suicide ideation/attempt	Emergent	Evaluation for an underlying issue such as battery life and/or unintended on/off. Admit the patient to the hospital for multidisciplinary care including behavioral therapy, counseling, medication adjustment and/or stimulation adjustment.
Air embolus	Emergent	Wax edges of the burr hole, lower patient's head, jugular venous compression, administer oxygen
Infection-UTI	Routine/urgent	Hydration and appropriate antibiotics, case should be taken to adjust PD medications if necessary as levels may be altered by antibiotics.
Infection-lead	Emergent	The lead should be removed and appropriate antibiotics should be administered.
Infection-IPG	Urgent	The IPG and usually the extension cable should be removed and appropriate antibiotics should be administered.
Lead fracture	Urgent	Lead replacement, if an appropriate candidate.
Lead electrical short	Urgent	Lead replacement, or potentially reprogramming at a different contact.
Lead migration	Urgent	Lead replacement, surgical alteration of lead position, or potentially reprogramming at a different contact.
Lead misplacement	Urgent	Lead replacement.
IPG malfunction	Urgent	IPG replacement, manage potential rebound symptoms.

the patient died in his sleep on postoperative day one from a myocardial infarction.

Assessment of medical comorbidities must be performed on all patients undergoing DBS surgery [21]. Clinicians should be aware that patients taking medications that can affect the cardiovascular system such as bromocriptine, and tricyclic antidepressants (TCAs) may be at increased risk when undergoing general anesthesia [36]. The incidence of angina and arrhythmia following DBS surgery has been reported as 0.3% in a recent large single center study [20]. A history of CAD may increase the perioperative risk of MI and angina. High risk patients should be carefully monitored (pre and postoperatively), and they may even require extra monitoring following general anesthesia. Cardiac or pulmonary symptoms in the postoperative period should be treated as an urgent, and possibly even emergent complications. Although this complication can be encountered following any surgical procedure, chest pain in the region surrounding the IPG DBS skin incision may be erroneously attributed to a DBS-related issue rather than to a cardiac related issue [37]. Clinicians should be aware that the risk of comorbidities and medications, and that postoperative chest pain following DBS/IPG implantation can present or evolve into urgent or emergent issues.

2.1.7. Air embolus

Air embolus a relatively uncommon complication of neurosurgical procedures. However, clinicians should be aware that the incidence of air embolus during DBS surgeries has been reported to be as high as 3% in a recent report, and DBS-related air embolus may manifest differently from other neurosurgical procedures, since during DBS the procedure is performed awake rather than under general anesthesia [38,39]. When the neurosurgeon is preparing the burr hole for microelectrode recording and/or macrostimulation, air embolus may occur with tachycardia, a rise in the end tidal CO_2, and cough. This reaction is typical of entrainment of air into the venous system. It is important to preoperatively position the patient's head as close to supine as possible to minimize this complication. In a recent series, Hooper et al. reported the potential use of an external Doppler device to enhance monitoring for air embolus during DBS [39]. These authors also noted that the cough was the best clinical indicator to pick up an air embolus. When encountered, the head position should be adjusted (lower the patient's head), bone edges of the burr hole should be waxed, the surgical field rigorously irrigated, and the patient vigorously supported from a cardiopulmonary standpoint. Additionally, having the neurologist, nurse or physiologist temporarily compress the neck (to inhibit venous return) may aid the neurosurgeon in identifying the problematic region, and in quickly correcting the situation (Table 1).

2.2. Hardware-related urgencies/emergencies

2.2.1. Hardware infection

Case 5. A 43-year-old man with a nine-year-history of PD underwent unilateral STN DBS. He arrived for a routine clinic appointment and staple removal on postoperative day seventeen. Following the staple removal there was purulent drainage from the cranial incision site, and the pectoral incision revealed tender erythema (Fig. 2). He was admitted to the hospital urgently, and the IPG and the extension wire were both removed. A course of intravenous antibiotics was completed prior to re-implantation.

Case 6. A 71-year-old man with a history of medically refractory essential tremor (ET) underwent a unilateral thalamic DBS implantation. Four weeks following surgery, the patient reported to the clinic for routine follow up care. Headache and progressive dysphagia were the chief complaints, and a head CT scan revealed a brain abscess along the DBS lead tract. The CT scan demonstrated an edematous lesion surrounding the DBS lead which was enhanced with contrast media (Fig. 3). He was admitted for emergent craniotomy, DBS lead removal and abscess drainage.

Hardware related infections are not uncommon in DBS. The incidence of infection and/or erosion following device implantations has been reported to range between 0 and 15.2% [10,40–46]. Even the most vigilant surgical technique cannot guarantee the absence of postoperative infectious complications. The devices in these scenarios may require emergent removal, in contrast to the management of ICH, which may not require lead removal (Table 1). Cultures should be sent anytime hardware is removed or a potentially infectious pocket aspirated. Although several factors may be related to infection rate, pre and postoperative prophylactic antibiotics may prevent hardware infection, however the evidence base for their use is

Fig. 2. Infection in the cranial skin incision. The illustration reveals purulent drainage from the cranial incision.

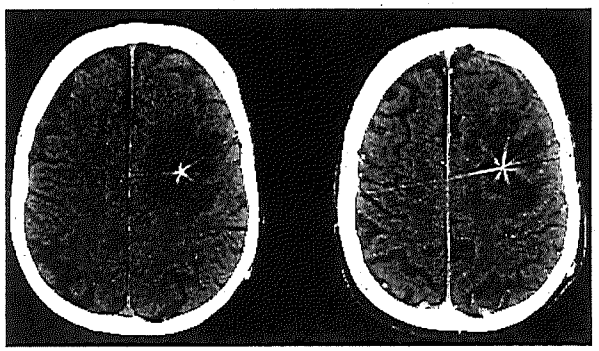

Fig. 3. Computed tomography (CT) scan images of a brain abscess following DBS lead implantation. A CT scan image without contrast (left) revealed a low density area which indicated an edematous lesion surrounding the DBS lead. The lesion was enhanced with contrast media (right).

weak [44,46]. One recent study did however report a reduction in the infection rate by locally injecting anti-staphylococcal antibiotics (e.g. neomycin, polymixin) directly into the operative wound [46].

There are several factors that may impact the management of a DBS infection. These include 1 – whether the infection is deep or superficial, 2 – whether the brain lead is involved, and 3 – whether there are single or multiple sites of involvement [40]. A superficial infection may be managed in select cases in a non-operative and conservative fashion, however a deep infection may require emergent hardware removal. When the brain lead and/or multiple sites are involved, many DBS teams elect to remove all hardware (lead, extension, and IPG). In cases where only the IPG or extension cable appears infected, there is an option to remove only the purported infected hardware and to attempt to preserve the brain lead. Following a course of 6–8 weeks of IV antibiotic therapy, device(s) re-implantation may be possible.

2.2.2. Hardware malfunction

Case 7. A 76-year-old woman with a history of essential tremor (ET) who underwent a left thalamic DBS implantation three years prior presented to clinic with sudden tremor recurrence. A few days before her presentation, following a mammogram she experienced a tingling sensation in the right upper extremity with an abrupt loss of benefit in her right upper extremity tremor. When the device was checked the impedance was discovered to be greater than 2000 Ω, and a chest x-ray revealed a flipped IPG and a twisted extension cable (Fig. 4). A fracture of the extension cable was suspected, and replacement of the cable resolved the issue.

When a DBS patient reports sudden loss of efficacy, the clinician should consider hardware malfunction [4,47]. Mechanical stress to the device may result in lead fracture, a break in the extension cable, or an IPG failure. Blomstedt et al. reported 7 of 8 broken electrodes in their cases were encountered in patients with ET, and they speculated head tremor may have contributed to the adverse event(s) [44]. Compulsive manipulation of the IPG device, referred to as "Twiddler's syndrome", has also been reported to result in extension cable fractures [48].

The DBS programming/interrogation device should be used to measure the impedance and current drain for each of the four lead contacts. This procedure will assist in verifying the physical integrity of the DBS system. A high impedance along with a low current drain may be consistent with a lead fracture or with an extension cable break. Alternatively a low impedance with possible high current drain may be supporting evidence for a short circuit. In short circuits the patient will frequently complain of a shock-like sensation when palpating the IPG or when pressing along the extension cable tract. A plain film x-ray should be obtained to search for a fracture along the course of the lead or extension wire (Fig. 5). When the location of the problem cannot be precisely identified, the next step is to replace the extension wire and to retest impedances in the operating room setting. This procedure may save replacement of the intracranial lead in select cases [47]. Clinicians should always keep in mind that contacts with normal impedances/current

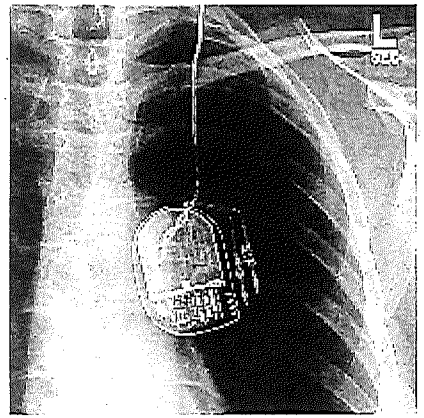

Fig. 4. A chest x-ray revealed a twisted extension cable and flipped IPG following a mammography. These features have been referred to as the twiddler syndrome.

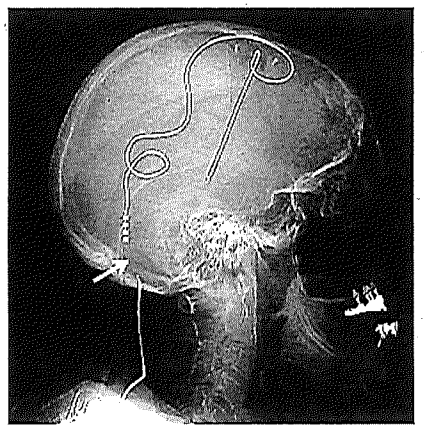

Fig. 5. A skull x-ray revealed an extension cable fracture.

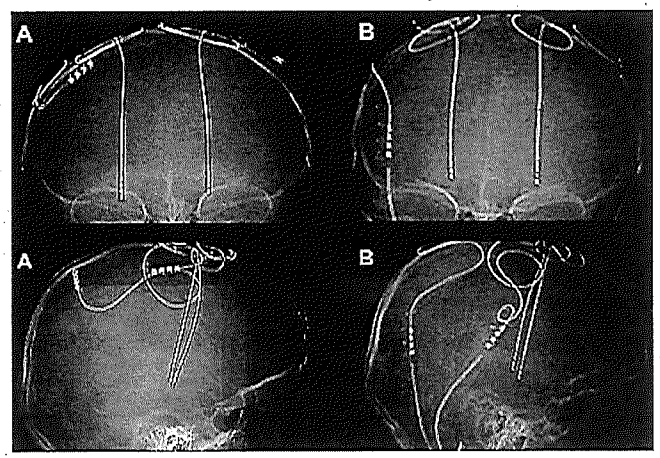

Fig. 6. Dorsal lead migration shown by serial x-rays. A) A skull x-ray at one month post-implantation. B) A skull x-ray at eight months pre-repeat implantation. Left and right leads had deviated from baseline.

drain values, are potentially programmable. An attempt to reprogram these functioning contacts should be sought prior to recommending replacement (Table 1).

2.2.3. Lead migration

Case 8. A 7-year-old boy with DYT-1 positive generalized dystonia underwent bilateral GPi DBS. After an initial dramatic response, his benefit deteriorated over the first year. Measurement and comparison of his DBS leads revealed dorsal lead migration (Fig. 6). His head circumference was measured and found to be 51.5 cm preoperatively and 53 cm 30 months later. Repositioning the DBS leads recaptured benefits.

Case 9. A 26-year-old man developed tardive dystonia following exposure to a neuroleptic drug used to address his severe depression. He subsequently underwent bilateral GPi DBS. Preoperatively he suffered severe and painful retrocollic head jerks. Postoperatively his subjective pain and head jerking clinically improved (pain approximately 50+% and movement disorders approximately 40–50%). Six months following the operation the benefits waned, and a CT scan revealed that the left and the right leads had migrated 15.6 mm and 4.6 mm ventrally from their initial position (Fig. 7). The patient underwent successful lead replacements.

Lead migration, either dorsal or ventral, can result from a malfunction of anchoring devices, skull growth, or vigorous head movements [47,49]. Yianni et al. reported that 3 of 133 patients (2.3%) experienced lead migration [49]. All three patients had dystonia, and the authors hypothesized that axial movements contributed to lead migration. When ventral lead migration is noted in a patient with GPi DBS, clinicians should be cautious as the ventral lead migration may result in severe mood changes due to the spread of the stimulation to other regions such as but not limited to the amygdala [50]. Skull growth in children is another cause of lead migration as illustrated by case 7. When lead migration is noted, changing the active contact (deeper or shallower depending on the direction of migration) should be attempted in most cases prior to surgical revision [51] (Table 1). This adverse event highlights the importance of examining postoperative imaging.

2.2.4. Lead misplacement

Case 10. A 60-year-old man with a history of PD underwent bilateral STN DBS at an outside institution 5 years prior to presentation to our clinic. He reported a lack of benefit from DBS, and repeated programming in the past had not improved his situation. An MRI scan revealed lead misplacement (Fig. 8). The patient was unwilling to undergo a lead replacement because of a combination of claustrophobia and fear of the surgical suite.

Lead misplacement is a not uncommon complication of DBS surgery and has been reported to be associated with technical error, intraoperative brain shift

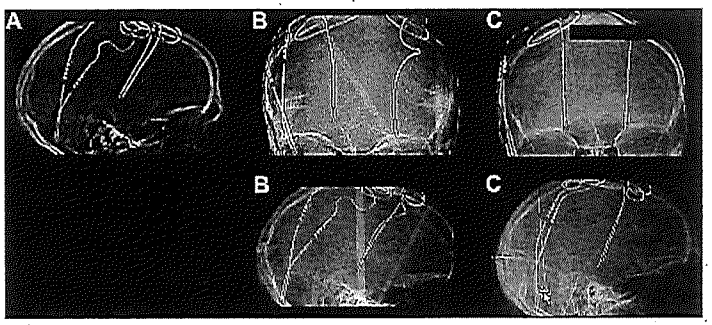

Fig. 7. Ventral lead migration shown by serial x-rays. A) A skull x-ray at one month post-implantation. B) A skull x-ray at fourteen months following first operation. The left and right leads had moved approximately 16 mm and 5 mm downwards from the initial position, respectively. C) A skull x-ray at one month following lead replacement.

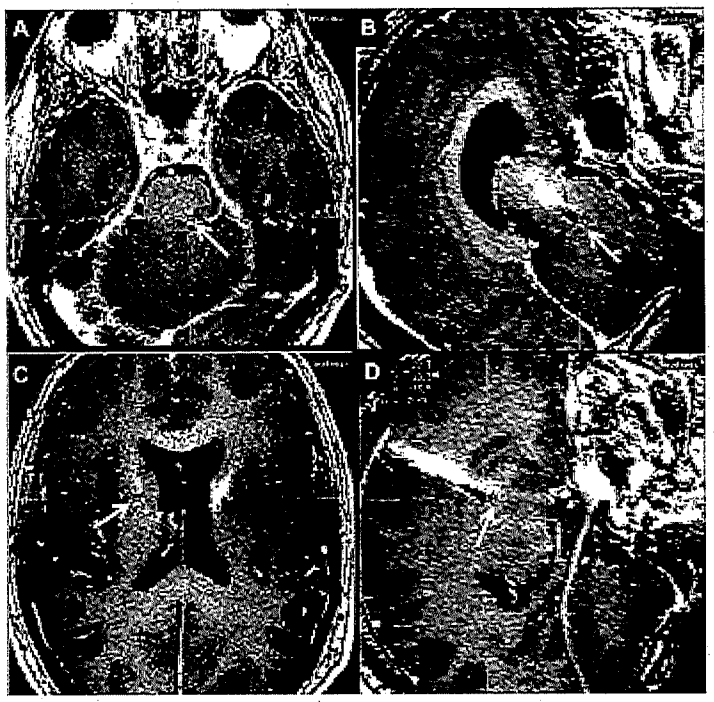

Fig. 8. Lead misplacement. Arrows indicate the tip of DBS leads. An axial slice (A) and a sagittal slice (B) of a T1 weighted magnetic resonance imaging (MRI) scan revealed the tip of the left DBS lead located too far posterior and deep for the subthalamic nucleus (STN). An axial slice (C) and a sagittal slice (D) of the same MRI scan revealed too shallow location of the left DBS lead.

(usually the result of a cerebrospinal fluid (CSF) leak [5]), and/or a failure in devices designed to secure the lead [49]. A suboptimal outcome from DBS surgery and/or low thresholds for stimulation-induced side effects (when the device is interrogated) may suggest lead misplacement. DBS leads placed in suboptimal locations may not be able to be corrected by programming [47]. Stimulation-induced side effects can lead to an urgent or an emergent situation, and in extreme cases can result in severe and sometimes unexpected symptoms. Even slight variations (sometimes only millimeters) of the location of a DBS lead may alleviate negative symptoms and lead to a more optimal therapeutic benefit [51] (Table 1).

2.3. Stimulation-related urgencies/emergencies

2.3.1. Stimulation-related motor symptoms

Stimulation-related motor symptoms include dyskinesia, chorea/ballism, gait disturbances, motor pulling, verbal fluency problems (verbal fluency has motor and non-motor/cognitive components), dysarthria, and hypophonia (Table 2). Many stimulation-induced motor symptoms resolve following reprogramming of the voltage, pulse width, and/or frequency.

If dyskinesia or chorea/ballism was induced by stimulation, reducing the amplitude/voltage of stimulation, or reducing the levodopa equivalent dose may alleviate the issue. Severe stimulation-induced dyskinesia/ballism in the clinic setting should alert the DBS programmer that voltage adjustment should be performed very slowly (sometimes in 0.1–0.2 V increment increases over many weeks). When stimulation-induced hyperkinesia is encountered, the ultimate outcome for patients is usually excellent. One important exception is underlying infection (e.g. pneumonia, UTI, etc.) which may exacerbate dyskinesia. We suggest an evaluation for an infectious process should be sought in cases where medical management proves difficult [18].

Although pre-existing gait and/or speech problems (e.g. on medication freezing, dysarthria, and hypophonia) do not typically respond to stimulation [23,52], stimulation-induced gait and speech issues may be improved in select cases with reprogramming, sometimes into a bipolar configuration. Patients themselves may discover relief by switching one or both devices (utilizing a remote control) to an off position when speaking. Additionally recent reports have revealed changing high frequency (>100 Hz) to lower frequency (<100 Hz) programming settings may improve gait, voice and other clinical features [53,54]. More research into DBS settings that may have the potential to improve or enhance clinical symptoms will be required, as some of the current low frequency settings seem to provide only temporary relief [53,54].

2.3.2. Stimulation-related non-motor symptoms

When stimulation spreads to surrounding neuronal regions, and to limbic and associative regions within grey matter structures, symptoms such as unpleasant feelings, paresthesias, behavioral complaints, and cognitive issues may emerge (Table 2). Pseudobulbar laughter and crying (mood incongruent) have been reported with stimulation, and both have been reportedly addressed by the use of antidepressant medications and by DBS reprogramming [55–57]. Two of the most worrisome stimulation-induced issues are depression and mania [32,58–62]. Both may require medication changes, reprogramming, verification of lead locations and potential hospitalization [47]. Depression should be carefully followed as it can result in suicidal ideation or suicidal attempt [32]. Several reports have linked stimulation of the substantia nigra region to acute depression in patients with STN DBS [58,59]. Abrupt cessation or reduction of dopaminergic medications can also result in apathy or depression [52,63]. If depression follows induction of stimulation, reprogramming to a more dorsal contact may be one solution. The lead location should be checked as misplacement into non-motor regions is one explanation for stimulation-induced non-motor features. Useful strategies include administration of antidepressants/antipsychotics, titrating neuropsychiatric medications to optimal doses, and completely optimizing dopaminergic medications [52]. Inpatient care including multi/interdisciplinary approaches (including psychiatrists, psychologists, neurologists, neurosurgeons and other health professionals) and behavioral therapies may also prove useful.

Table 2
Postoperative stimulation-induced urgencies and emergencies.

Issue	Routine/urgent/emergent	Management
Chorea/ballism	Routine/urgent	Try to program slowly (e.g. slow increase of voltage over many weeks/months). May try dorsal contact. May also reduce dopaminergic medications.
Dyskinesia	Routine/urgent	Reducing the dopaminergic medication may help. Try to program slowly (e.g. slow increase of voltage over many weeks/months). May try dorsal contact.
Motor pulling	Urgent	Try to reduce voltage or pulse width. Try bipolar stimulation, or possibly another lead contact. Some situations may require lead replacement. Check lead location.
Gait disturbance	Routine/urgent	Try another setting (e.g. another contact, reducing pulse width, voltage or frequency). Low frequency (60 Hz) with higher voltage or pulse width may help.
Verbal fluency problem	Routine	Try another contact, perhaps a more dorsal contact on the DBS lead. Try changing stimulation to bipolar or decrease pulse width, voltage or frequency.
Dysarthria/dysphagia	Routine	Try another contact. Try changing stimulation to bipolar or decrease pulse width, voltage or frequency. Check lead location. Prescribe speech therapy.
Hypophonia	Routine	Try another contact. Try changing stimulation to bipolar or decrease pulse width, voltage or frequency. Prescribe speech therapy.
Cognitive decline	Routine	This problem may be disease progression, surgery-related, or stimulation-related. Seek neuropsychological testing, consider reprogramming to a dorsal contact. Check lead location.
Mania/hypomania	Routine/urgent	Adjust medications. Consider discontinuation of dopamine agonist and use of quetiapine or clozapine. Consider moving to a dorsal contact and/or decreasing the pulse width, voltage or frequency. Check lead location. Consider admission for multi/interdisciplinary management.
Impulse control	Urgent	Adjust medications. Consider discontinuation of dopamine agonist and addition of clozaril or seroquel. Consider moving to a dorsal contact and/or decreasing the pulse width, voltage or frequency. Check lead location. Consider admission for multi/interdisciplinary management.
Suicide ideation/attempt	Emergent	Admit the patient to the hospital for multi/interdisciplinary care, and treat underlying cause. May need both medication adjustment and programming. Check lead location.
Anxiety/fear	Urgent	Consider more frequent and higher doses of dopaminergics, and altering DBS contacts, perhaps moving more dorsal. Check lead location. Consider admission for multi/interdisciplinary management.
Severe depression	Emergent	Behavioral therapy, counseling, medication adjustment and/or stimulation adjustment. Check lead location. Consider admission for multi/interdisciplinary management.
Postoperative mania	Urgent	Behavioral therapy, counseling, medication adjustment and/or stimulation adjustment. Check lead location. Consider admission for multi/interdisciplinary management.
Pseudobulbar cry/laughter	Urgent	SSRI, TCA or dextromethorphan.
Autonomic features	Urgent	May habituate on own, try stimulation parameter adjustments, or change contact if continues to be troublesome.
Sensory phenomena	Urgent	Try reduce voltage or pulse width. Try bipolar, or possibly other contact.
Accidental on/off	Urgent/emergent	Turn on the IPG, keep a diary to identify the problem.
Symptom rebound (motor and/or non-motor)	Emergent	DBS hardware workup including impedance check, battery check, x-ray study, and assess for tolerance.

2.3.3. Accidental on/off

When the DBS device unpredictably turns off, the clinician must investigate potential environmental triggers (the device has a duty log to assist in documenting these occurrences). Exposure to magnetic forces (e.g., a magnetized ice freezer or store security devices) is the most commonly reported etiology [47]. Prescribing "rechecking" of the DBS device on a regular or semi-regular schedule may prove useful (utilizing the patient issued remote control). Additionally, having the patient document and describe activities and relevant environments may yield the source of the problem. The patient should be educated to avoid strong magnetic fields, and to have their remote device with them at all times in order to recheck on/off status, and to learn prevention strategies for accidental on/off's. Most patients who undergo DBS surgery do not have any issues with accidental on/off's during the lifetime of their devices.

If more than one IPG is utilized to power multiple DBS leads, the chest pacemakers must be placed a minimum of six inches apart. Failure to separate the IPG's in space may result in cross-communication of the devices, and a result in an automatic and unintended reset to the factory default stimulation settings. We have observed this phenomenon in a single case, a boy with generalized dystonia and two chest IPGs (author observations). Interestingly when lying supine this boy's devices were six inches apart, but when leaning forward in a chair for programming sessions the distance was cut to only four inches. It is therefore important when programming to make sure (especially in children) that patients sit back in the chair, or alternatively lie in a supine position.

2.3.4. Symptom rebound

Several cases of severe symptom rebound following battery failure have been reported following DBS [64,65]. The more beneficial DBS is for clinical symptoms, the more dramatic the rebound symptoms may be. Symptom rebound may include both motor and non-motor manifestations such as tremor, gait problems, stiff legs and suicidal ideation (author observations), as well as severe depression. We have observed rebound of motor symptoms with battery failures in cases of dystonia and Parkinson's disease, but also rebound of non-motor symptoms including depression and suicidal ideation with battery failure (author observations). Sudden worsening of symptoms should always prompt a battery status check by an experienced DBS programmer. If the device is off, resuming stimulation may be all that is necessary (see Section 2.3.3). If the device is on, checking impedances and current drain at each of the four DBS contacts may provide useful information for evaluation of lead integrity (hardware malfunction) as discussed in the "hardware malfunction" section of this paper (Table 2).

3. Others

3.1. Dystonic storm

Dystonic storm or status dystonicus is a rare but possibly life-threatening condition which presents with severe generalized and possibly painful hyperkinetic dystonic spasms. Patients with an underlying history of primary or secondary dystonia are prone to this condition, and stressors such as trauma, infection or surgical intervention can trigger the dystonic spasms. The optimum treatment for this condition is not established, but a reasonable strategy is to use an aggressively increasing approach beginning with oral medications, then graduating to intravenous and intrathecal medications, then switching to deep sedation or anesthesia, and finally culminating with surgery [66]. Dopamine blockade with non-selective agents such as pimozide, risperidone, olanzapine or haloperidol and sedation with propofol and midazolam, have all been reported successful for the short term control of symptoms, and for improving quality of life. Manji et al. has reported that triple therapy with oral tetrabenazine, high-dose benzhexol, and pimozide is effective especially in children [67,68]. However, dystonic

storms may be unusually refractory to some oral medications. Patients with dystonic storms should be admitted to the intensive care unit (ICU) due to the possibility of accompanying respiratory compromise, hyperthermia, dehydration, and rhabdomyolysis resulting in potential renal failure. Deep sedation or anesthesia with endotracheal intubation may be required for refractory cases. Additionally, there has been at least one case of a patient with a dystonic storm successfully treated with intrathecal baclofen [69]. DBS or pallidotomy may be an option of last resort in cases where symptoms continue for many weeks/months [70,71]. Clinicians should be aware that postoperative infections and certain medications (dopamine blockers, antiemetics, etc.) can postoperatively induce movement disorders especially in patients with pre-existing basal ganglia damage.

4. Conclusion

Knowledge of potential DBS urgencies and emergencies can in many cases enhance outcomes. More intra- and postoperative urgencies and emergencies continue to be identified as the DBS field expands. Clinician's handling DBS in their practices should be versed in the identification and management of surgery/procedure related, hardware related, and stimulation-induced issues.

References

[1] Anderson WS, Lenz FA. Surgery insight: deep brain stimulation for movement disorders. Nat Clin Pract Neurol 2006;2:310–20.
[2] Hariz MI. Psychosurgery, deep brain stimulation, and the re-writing of history. Neurosurgery 2008;63:E820. author reply E820.
[3] Hooper AK, Ellis TM, Foote KD, Zeilman P, Okun MS. Dyskinetic storm induced by intra-operative deep brain stimulator placement. Open Neurosurg J 2009; 2:1–3.
[4] Deuschl G, Herzog J, Kleiner-Fisman G, Kubu C, Lozano AM, Lyons KE, et al. Deep brain stimulation: postoperative issues. Mov Disord 2006;21(Suppl. 14): S219–37.
[5] Hariz MI. Complications of deep brain stimulation surgery. Mov Disord 2002;17(Suppl. 3):S162–6.
[6] Hariz MI, Fodstad H. Do microelectrode techniques increase accuracy or decrease risks in pallidotomy and deep brain stimulation? A critical review of the literature. Stereotact Funct Neurosurg 1999;72:157–69.
[7] Binder DK, Rau GM, Starr PA. Risk factors for hemorrhage during microelectrode-guided deep brain stimulator implantation for movement disorders. Neurosurgery 2005;56:722–32. discussion 722–32.
[8] Pollak P, Krack P, Fraix V, Mendes A, Moro E, Chabardes S, et al. Intraoperative micro- and macrostimulation of the subthalamic nucleus in Parkinson's disease. Mov Disord 2002;17(Suppl. 3):S155–61.
[9] Sansur CA, Frysinger RC, Pouratian N, Fu KM, Bittl M, Oskouian RJ, et al. Incidence of symptomatic hemorrhage after stereotactic electrode placement. J Neurosurg 2007;107:998–1003.
[10] Beric A, Kelly PJ, Rezai A, Sterio D, Mogilner A, Zonenshayn M, et al. Complications of deep brain stimulation surgery. Stereotact Funct Neurosurg 2001; 77:73–8.
[11] Lyons KE, Wilkinson SB, Overman J, Pahwa R. Surgical and hardware complications of subthalamic stimulation: a series of 160 procedures. Neurology 2004;63:612–6.
[12] Videnovic A, Metman LV. Deep brain stimulation for Parkinson's disease: prevalence of adverse events and need for standardized reporting. Mov Disord 2008;23:343–9.
[13] Gorgulho A, De Salles AA, Frighetto L, Behnke E. Incidence of hemorrhage associated with electrophysiological studies performed using macroelectrodes and microelectrodes in functional neurosurgery. J Neurosurg 2005;102: 888–96.
[14] Voges J, Hilker R, Botzel K, Kiening KL, Kloss M, Kupsch A, et al. Thirty days complication rate following surgery performed for deep-brain-stimulation. Mov Disord 2007;22:1486–9.
[15] Morishita T, Burdick A, Okun MS, Jacobson C, Foote KD. Cerebral venous infarction: an avoidable complication of deep brain stimulation surgery. In: 13th international congress of Parkinson's disease and movement disorders. Paris; 2009.
[16] Umemura A, Jaggi JL, Hurtig HI, Siderowf AD, Colcher A, Stern MB, et al. Deep brain stimulation for movement disorders: morbidity and mortality in 109 patients. J Neurosurg 2003;98:779–84.
[17] Kipps CM, Fung VS, Grattan-Smith P, de Moore GM, Morris JG. Movement disorder emergencies. Mov Disord 2005;20:322–34.
[18] Factor SA, Molho ES. Emergency department presentations of patients with Parkinson's disease. Am J Emerg Med 2000;18:209–15.
[19] Herzog J, Pinsker M, Wasner M, Steigerwald F, Wailke S, Deuschl G, et al. Stimulation of subthalamic fibre tracts reduces dyskinesias in stn-dbs. Mov Disord 2007;22:679–84.
[20] Kenney C, Simpson R, Hunter C, Ondo W, Al maguer M, Davidson A, et al. Short-term and long-term safety of deep brain stimulation in the treatment of movement disorders. J Neurosurg 2007;106:621–5.
[21] Rodriguez RL, Fernandez HH, Haq I, Okun MS. Pearls in patient selection for deep brain stimulation. Neurologist 2007;13:253–60.
[22] Anderson VC, Burchiel KJ, Hogarth P, Favre J, Hammerstad JP. Pallidal vs subthalamic nucleus deep brain stimulation in Parkinson disease. Arch Neurol 2005;62:554–60.
[23] Okun MS, Fernandez HH, Wu SS, Kirsch-Darrow L, Bowers D, Bova F, et al. Cognition and mood in Parkinson's disease in subthalamic nucleus versus globus pallidus interna deep brain stimulation: the compare trial. Ann Neurol 2009.
[24] Okun MS, Green J, Saben R, Gross R, Foote KD, Vitek JL. Mood changes with deep brain stimulation of stn and gpi: results of a pilot study. J Neurol Neurosurg Psychiatry 2003;74:1584–6.
[25] Hariz MI, Rehncrona S, Q uinn NP, Speelman JD, Wensing C. Multicenter study on deep brain stimulation in Parkinson's disease: an independent assessment of reported adverse events at 4 years. Mov Disord 2008; 23:416–21.
[26] Tune LE, Damlouji NF, Holland A, Gardner TJ, Folstein MF, Coyle JT. Association of postoperative delirium with raised serum levels of anticholinergic drugs. Lancet 1981;2:651–3.
[27] Poewe W. When a Parkinson's disease patient starts to hallucinate. Pract Neurol 2008;8:238–41.
[28] Frucht SJ. Movement disorder emergencies in the perioperative period. Neurol Clin 2004;22:379–87.
[29] Poston KL, Frucht SJ. Movement disorder emergencies. J Neurol 2008; 255(Suppl. 4):2–13.
[30] Foncke EMJ, Schuurman PR, Speelman JD. Suicide after deep brain stimulation of the internal globus pallidus for dystonia. Neurology 2006;66:142–3.
[31] Burkhard PR, Vingerhoets FJG, Berney A, Bogouss lavsky J, Villemure JG, Ghika J. Suicide after successful deep brain stimulation for movement disorders. Neurology 2004;63:2170–2.
[32] Doshi PK, Chhaya N, Bhatt MH. Depression leading to attempted suicide after bilateral subthalamic nucleus stimulation for Parkinson's disease. Mov Disord 2002;17:1084–5.
[33] Voon V, Krack P, Lang AE, Lozano AM, Dujardin K, Schupbach M, et al. A multicentre study on suicide outcomes following subthalamic stimulation for Parkinson's disease. Brain 2008;131:2720–8.
[34] Okun MS, Rodriguez RL, Mikos A, Miller K, Kellison I, Kirsch-Darrow L, et al. Deep brain stimulation and the role of the neuropsychologist. Clin Neuropsychol 2007;21:162–89.
[35] Ghika J, Villemure JG, Miklossy J, Temperli P, Pralong E, Christen-Zaech S, et al. Postanoxic generalized dystonia improved by bilateral voa thalamic deep brain stimulation. Neurology 2002;58:311–3.
[36] Burton DA, Nicholson G, Hall GM. Anaesthesia in elderly patients with neurodegenerative disorders: special considerations. Drugs Aging 2004;21: 229–42.
[37] Resnick AS, Foote KD, Rodriguez RL, Malaty IA, Moll JL, Carden DL, et al. The number and nature of emergency department encounters in patients with deep brain stimulators. J Neurol, in press. doi:10.1007/s00415-009-5343-8. Published online 8 October 2009.
[38] Deogaonkar A, Avitsian R, Henderson JM, Schubert A. Venous air embolism during deep brain stimulation surgery in an awake supine patient. Stereotact Funct Neurosurg 2005;83:32–5.
[39] Hooper AK, Okun MS, Foote KD, Haq IU, Fernandez HH, Hegland D, et al. Venous air embolism in deep brain stimulation. Stereotact Funct Neurosurg 2009;87:25–30.
[40] Sillay KA, Larson PS, Starr PA. Deep brain stimulator hardware-related infections: incidence and management in a large series. Neurosurgery 2008;62:360–6. discussion 366–7.
[41] Joint C, Nandi D, Parkin S, Gregory R, Aziz T. Hardware-related problems of deep brain stimulation. Mov Disord 2002;17(Suppl. 3):S175–80.
[42] Kondziolka D, Whiting D, Germanwala A, Oh M. Hardware-related complications after placement of thalamic deep brain stimulator systems. Stereotact Funct Neurosurg 2002;79:228–33.
[43] Oh MY, Abosch A, Kim SH, Lang AE, Lozano AM. Long-term hardware-related complications of deep brain stimulation. Neurosurgery 2002;50:1268–74. discussion 1274–6.
[44] Blomstedt P, Hariz MI. Hardware-related complications of deep brain stimulation: a ten year experience. Acta Neurochir (Wien) 2005;147:1061–4. discussion 1064.
[45] Koller W, Pahwa R, Busenbark K, Hubble J, Wilkinson S, Lang A, et al. High-frequency unilateral thalamic stimulation in the treatment of essential and parkinsonian tremor. Ann Neurol 1997;42:292–9.
[46] Miller JP, Acar F, Burchiel KJ. Significant reduction in stereotactic and functional neurosurgical hardware infection after local neomycin/polymyxin application. J Neurosurg 2009;110:247–50.
[47] Okun MS, Rodriguez RL, Foote KD, Sudhyadhom A, Bova F, Jacobson C, et al. A case-based review of troubleshooting deep brain stimulator issues in movement and neuropsychiatric disorders. Parkinsonism Relat Disord 2008;14: 532–8.

[48] Geissinger G, Neal JH. Spontaneous twiddler's syndrome in a patient with a deep brain stimulator. Surg Neurol 2007;68:454–6. discussion 456.
[49] Yianni J, Nandi D, Shad A, Bain P, Gregory R, Aziz T. Increased risk of lead fracture and migration in dystonia compared with other movement disorders following deep brain stimulation. J Clin Neurosci 2004;11:243–5.
[50] Piacentini S, Romito L, Franzini A, Granato A, Broggi G, Albanese A. Mood disorder following dbs of the left amygdaloid region in a dystonia patient with a dislodged electrode. Mov Disord 2008;23:147–50.
[51] Ellis TM, Foote KD, Fernandez HH, Sudhyadhom A, Rodriguez RL, Zeilman P, et al. Reoperation for suboptimal outcomes after deep brain stimulation surgery. Neurosurgery 2008;63:754–60. discussion 760–1.
[52] Krack P, Batir A, Van Blercom N, Chabardes S, Fraix V, Ardouin C, et al. Five-year follow-up of bilateral stimulation of the subthalamic nucleus in advanced Parkinson's disease. N Engl J Med 2003;349:1925–34.
[53] Moreau C, Defebvre L, Destee A, Bleuse S, Clement F, Blatt JL, et al. Stn-dbs frequency effects on freezing of gait in advanced Parkinson disease. Neurology 2008;71:80–4.
[54] Brozova H, Barnaure I, Alterman RL, Tagliati M. Stn-dbs frequency effects on freezing of gait in advanced Parkinson disease. Neurology 2009;72:770. author reply 770–1.
[55] Low HL, Sayer FT, Honey CR. Pathological crying caused by high-frequency stimulation in the region of the caudal internal capsule. Arch Neurol 2008; 65:264–6.
[56] Okun MS, Raju DV, Walter BL, Juncos JL, DeLong MR, Heilman K, et al. Pseudobulbar crying induced by stimulation in the region of the subthalamic nucleus. J Neurol Neurosurg Psychiatry 2004;75:921–3.
[57] Kumar R, Krack P, Pollak P. Transient acute depression induced by high-frequency deep-brain stimulation. N Engl J Med 1999;341:1003–4. author reply 1004.
[58] Blomstedt P, Hariz MI, Lees A, Silberstein P, Limousin P, Yelnik J, et al. Acute severe depression induced by intraoperative stimulation of the substantia nigra: a case report. Parkinsonism Relat Disord 2008;14:253–6.
[59] Bejjani BP, Damier P, Arnulf I, Thivard L, Bonnet AM, Dormont D, et al. Transient acute depression induced by high-frequency deep-brain stimulation. N Engl J Med 1999;340:1476–80.
[60] Miyawaki E, Perlmutter JS, Troster AI, Videen TO, Koller WC. The behavioral complications of pallidal stimulation: a case report. Brain Cogn 2000;42: 417–34.
[61] Romito LM, Raja M, Daniele A, Contarino MF, Bentivoglio AR, Barbier A, et al. Transient mania with hypersexuality after surgery for high frequency stimulation of the subthalamic nucleus in Parkinson's disease. Mov Disord 2002;17:1371–4.
[62] Krack P, Kumar R, Ardouin C, Dowsey PL, McVicker JM, Benabid AL, et al. Mirthful laughter induced by subthalamic nucleus stimulation. Mov Disord 2001;16:867–75.
[63] Bejjani BP, Dormont D, Pidoux B, Yelnik J, Damier P, Arnulf I, et al. Bilateral subthalamic stimulation for Parkinson's disease by using three-dimensional stereotactic magnetic resonance imaging and electrophysiological guidance. J Neurosurg 2000;92:615–25.
[64] Hariz MI, Johansson F. Hardware failure in parkinsonian patients with chronic subthalamic nucleus stimulation is a medical emergency. Mov Disord 2001;16:166–8.
[65] Hariz MI, Shamsgovara P, Johansson F, Hariz G, Fodstad H. Tolerance and tremor rebound following long-term chronic thalamic stimulation for parkinsonian and essential tremor. Stereotact Funct Neurosurg 1999;72:208–18.
[66] Mariotti P, Fasano A, Contarino MF, Della Marca G, Piastra M, Genovese O, et al. Management of status dystonicus: our experience and review of the literature. Mov Disord 2007;22:963–8.
[67] Vaamonde J, Narbona J, Weiser R, Garcia MA, Brannan T, Obeso JA. Dystonic storms: a practical management problem. Clin Neuropharmacol 1994;17: 344–7.
[68] Manji H, Howard RS, Miller DH, Hirsch NP, Carr L, Bhatia K, et al. Status dystonicus: the syndrome and its management. Brain 1998;121(Pt. 2):243–52.
[69] Dalvi A, Fahn S, Ford B. Intrathecal baclofen in the treatment of dystonic storm. Mov Disord 1998;13:611–2.
[70] Elkay M, Silver K, Penn RD, Dalvi A. Dystonic storm due to batten's disease treated with pallidotomy and deep brain stimulation. Mov Disord 2009;24:1048–53.
[71] Teive HA, Munhoz RP, Souza MM, Antoniuk SA, Santos ML, Teixeira MJ, et al. Status dystonicus: study of five cases. Arq Neuropsiquiatr 2005;63:26–9.